Risky Inflation: A Cross Country Analysis

Jongrim Ha, Haroon Mumtaz, Franz Ruch

Working Paper No. 1004 July 2026 ISSN 1473-0278

School of Economics and Finance

Queen Mary
University of London

Risky Inflation: A Cross Country Analysis*

Jongrim Ha[1], Haroon Mumtaz[2], and Franz Ruch[1]

[1]World Bank
[2]Queen Mary University of London

This version: July 10, 2026.

Abstract

We develop a new dynamic factor model with stochastic volatility to quantify inflation tail risk across a large cross section of countries. The framework accommodates unbalanced panels and mixed-frequency data, allowing estimation of the full predictive distribution of inflation for over 200 economies over 1971–2023. Inflation risk—defined as the probability that inflation exceeds 5 percent over a twelve-month horizon—declined during the Great Moderation but rose sharply following the COVID-19 pandemic, with the global probability surpassing 50 percent from early 2021 through 2023. Exploiting the joint predictive distribution of inflation and real activity, we document a brief surge in global stagflation risk in late 2021. While inflation risk responds to both structural demand and supply shocks, it tends to decline during monetary policy tightening cycles. Cross-country evidence further shows that economies with greater trade and financial openness, stronger monetary policy frameworks, and fixed exchange rate regimes face systematically lower inflation risk, while commodity-exporting countries exhibit higher tail exposures. Overall, the results underscore the importance of monitoring inflation risks alongside inflation forecasts and highlight the role of institutions in mitigating macroeconomic tail vulnerabilities.

JEL Classification: C32; E44; E52.
Keywords: Monetary Policy; Risk; FAVAR; Stochastic Volatility.

*Corresponding author: Haroon Mumtaz (h.mumtaz@qmul.ac.uk). The views expressed herein are those of the authors and do not necessarily reflect those of the World Bank, its Executive Directors, or the countries they represent. The authors declare that they have no relevant or material financial interests that relate to the research described in this paper. No financial support to declare.

1 Introduction

Expectations about future inflation are a key input for policy decisions, whether in determining interest rates by monetary authorities or for designing fiscal measures. While much of the focus has traditionally been on forecasting the level of future inflation, policymakers are increasingly concerned with the evolution of uncertainty and the risks surrounding point forecasts. Recent developments in econometric modeling–including quantile regressions and stochastic volatility VARs–have highlighted the time-varying nature of uncertainty and the asymmetric behavior of tail outcomes. For example, López-Salido and Loria (2024) use the quantile regression methodology of Adrian et al. (2019) to show that the tails of the inflation forecast distribution vary substantially over time, a feature they label as inflation-at-risk (IAR).[1]

Much of the existing research on inflation tail risks has concentrated on advanced economies, notably the United States and the euro area. In our study, we adopt a methodology that enables us to characterize inflation tail risks across a broad set of countries simultaneously. This approach allows us to explore how inflation risks differ among economies with varying structural and macroeconomic characteristics. We define inflation risk as the probability that consumer price inflation over the next twelve months will exceed 5 percent, capturing the right-tail risk of the inflation distribution.

The proposed model builds on the dynamic factor model (DFM) developed by Caldara et al. (2024). In their framework, the standard DFM is extended to incorporate endogenous stochastic volatility, following approaches such as Mumtaz and Zanetti (2013); Creal and Wu (2017); Mumtaz (2018); Shin and Zhong (2020). In this setup, shocks to the latent factors can simultaneously affect both their means and volatilities, giving rise to rich dynamics in the conditional distributions of observable variables, which load onto these factors with varying intensities. While Caldara et al. (2024) apply their model to balanced panel datasets, we extend the framework to accommodate cross-country data characterized by missing observations and mixed-frequency variables.

Our results indicate that inflation risk increased markedly during the recent pandemic, with the predictive distribution of inflation shifting to the right beginning in March 2021. At that point, the probability that global consumer inflation would exceed 5 percent rose above 50 percent and remained elevated through April 2023. In March 2021, global consumer inflation stood at 3.7 percent. Around the same time, the Federal Reserve's April 2021 statement noted that "inflation has risen, largely reflecting transitory factors."

[1]Recent work has characterized similar risk dynamics for GDP growth (Adrian et al., 2019) and unemployment (Kiley, 2022).

Similarly, projections from the June 2021 FOMC anticipated median PCE inflation of 3.4 percent for 2021 and 2.1 percent for 2022. However, global inflation surpassed 5 percent by October 2021. The last instance when the probability of inflation exceeding 5 percent was above 50 percent occurred more than a decade earlier during the 2008–09 period, and more persistently throughout the 1980s and 1990s. We also find that inflation risk increased substantially across most world regions during the pandemic. The model's global coverage–encompassing over 200 economies–enables detailed country- and region-specific analyses of inflation risk dynamics.

The estimates can also be employed to evaluate stagflation risk, defined as the joint occurrence of one-year-ahead inflation exceeding 5 percent and negative industrial production growth. At the global level, the probability of stagflation surpassed 50 percent in October 2021, although this episode proved short-lived. The last period when a stagflation outcome was more likely than not occurred in the mid-1990s.

We apply the proposed measures of inflation risk along several dimensions to better understand its time-varying behavior and cross-regional and country heterogeneity. We first examine how inflation risk responds to macroeconomic disturbances. Using simulation-based impulse responses, we find that both demand- and supply-type shocks increase inflation tail risk across regions, although their relative importance varies geographically. In particular, supply-side disturbances generate larger increases in inflation risk in Europe, Africa, and Oceania, while demand shocks account for a greater share of overall variation in inflation risk in most regions.

On top of the role of cyclical structural shocks and policy variables on inflation risk, we examine how various slow-moving country characteristics–both related to monetary policy frameworks (such as central bank independence and the adoption of inflation targeting) and structural economic factors (including trade and financial openness)–are associated with inflation risk. Our findings suggest that economies with higher degrees of trade and capital account openness tend to experience lower inflation risk. Conversely, inflation risk is higher among commodity-exporting countries. The adoption of inflation-targeting regimes is associated with a reduction in inflation risk, though this effect is statistically significant only for advanced economies. Moreover, countries with greater central bank independence and transparency exhibit significantly lower inflation risk. Inflation risk also tends to decline during monetary policy tightening cycles. Finally, countries operating under fixed exchange rate regimes display systematically lower inflation risk. These results are broadly consistent with the existing literature on inflation and inflation risk.

Related literature. Forecasting the mean (and to a lesser extent dispersion) of inflation had traditionally been the primary focus of the literature (see, for example, Stock and Watson, 1999 on point forecasts, and Engle, 1982 on modeling volatility). However, as inflation declined during the Great Moderation and began undershooting central bank targets after the Global Financial Crisis (GFC), increasing attention shifted toward forecasting the entire distribution of inflation, moving beyond just the first two moments. In particular, the focus on inflation risk–the probability mass in the tails of the distribution–emerged in response to repeated episodes of low inflation and the perceived risk of deflation, such as Japan's experience in the 1990s, the aftermath of the Dot-Com Bust and 2001 recession, and the GFC and euro area debt crisis. These concerns played a role in motivating central banks to adopt unconventional monetary policies designed to minimize deflation risk.

Early contributions formalized ways to measure deflation risk. Diebold et al. (1997) evaluated the density forecasts of future inflation provided by the U.S. Survey of Professional Forecasters, revealing that the probability of large negative inflation shocks was generally overestimated, and that inflation surprises exhibit serial correlation. Kilian and Manganelli (2007) introduced a loss-function-based framework that used forecast errors to assess risks to price stability, finding little evidence of deflation risk for the United States and Germany but significant concerns in Japan. Building on this, Kitsul and Wright (2013) exploited quotes from inflation-linked options, specifically caps and floors, to estimate the entire probability distribution of future U.S. inflation. They showed that options-implied distributions assigned substantially more weight to extreme outcomes than traditional time-series models and indicated significant deflation risk after the GFC. These insights were reinforced by market-based studies: Christensen et al. (2016) developed a term structure model with stochastic volatility using Treasury inflation-protected securities (TIPS) and estimated that the probability of inflation averaging below 1 percent over a three-year horizon was close to unity immediately after the crisis and remained above 50 percent for years. Similarly, Fleckenstein et al. (2017) used inflation swaps and options to construct a simple market-based measure of inflation risk, finding probabilities of deflation above 10 percent at a two-year horizon. Deflation risk briefly re-emerged during the COVID-19 pandemic (Christensen et al., 2020).

While deflation dominated concerns in the 2000s and 2010s, the inflation landscape shifted dramatically after the pandemic, when consumer prices in advanced economies rose at rates not seen in four decades. This reversal shifted attention from the left to the right tail of the distribution. López-Salido and Loria (2024) studied tail risks of inflation using a quantile regression version of the Phillips curve for a panel of OECD countries.[2] They found that asymmetries in inflation outcomes—especially large increases in prices—were driven primarily by financial conditions, and to a lesser extent by labor market slack and oil prices. Complementing this econometric approach, Hilscher et al. (2024) used inflation swap contracts in the United States and Eurozone to estimate the tail probabilities of both very high and very low inflation, which they termed "inflation disasters," with a particular focus on long-horizon risks embedded in options prices.

These contributions reflected a broader methodological evolution in how inflation risk had been studied. Forecast-based measures such as those in Kilian and Manganelli (2007) were gradually complemented by market-based approaches that relied on information from options, TIPS, and swaps (Kitsul and Wright, 2013; Christensen et al., 2016; Fleckenstein et al., 2017; Hilscher et al., 2024). At the same time, quantile regression allowed researchers to capture shifting conditional distributions, providing a more flexible econometric tool for assessing the drivers of risks. More recently, machine learning methods–including quantile regression forests–have been applied to capture nonlinearities and improve density forecasts of inflation (Lenza et al., 2025). Studies on the disagreement in inflation expectations, such as Mankiw et al. (2003), also provided insights into the perceived uncertainty and width of the forecast distribution.

Empirical analyses of inflation risk have recently expanded to emerging market and developing economies (EMDEs). Banerjee et al. (2024) applied quantile Phillips curves across advanced and emerging economies, revealing that exchange rate depreciation and tighter financial conditions significantly elevated upside inflation risks in EMDEs; the latter also affecting deflation risks in EMDEs. Garrón et al. (2024) developed measures of inflation- and deflation-at-risk using factor-augmented quantile regressions and found that inflation vulnerabilities to global factors varied systematically across income groups.

This paper makes three contributions to the existing literature. First, it provides the first comprehensive global analysis of inflation tail risk using a unified density-based framework. Second, it extends stochastic-volatility dynamic factor models to unbalanced, mixed-frequency international panels, enabling risk measurement in data-poor settings. Third, it documents how structural and policy frameworks influence inflation risk, not merely inflation outcomes, offering new insights into the sources of macroeconomic vulnerability. Together, these findings underscore the importance of monitoring inflation risks alongside inflation forecasts and highlight the role of credible policy institutions in

[2] Queyranne et al. (2022) did the same for countries in the Middle East, North Africa, and Central Asia.

mitigating tail vulnerabilities.

The paper proceeds as follows. Sections 2 and 3 present the econometric framework and describe the data. Section 4 documents the evolution of inflation risk at the global and regional levels and introduces the analysis of stagflation risk based on the joint distribution of inflation and real activity. Section 5 examines the drivers of inflation risk, focusing on the response to macroeconomic demand and supply shocks as well as the role of monetary policy tightening cycles. Section 6 studies cross-country differences in inflation risk and relates them to structural characteristics, monetary policy frameworks, and exchange rate regimes. Section 7 reports robustness checks, and Section 8 concludes.

2 A Factor Model with Stochastic Volatility

In this section, we first present the econometric model and explain key features and assumptions. We continue by presenting the estimation algorithm and the data utilized in the application of the paper.

2.1 The Model

Following Caldara et al. (2024), we consider the following state-space model:

$$X_t = B_f f_t + B_z z_t + v_t \tag{1}$$

$$F_t = c + \sum_{j=1}^{P} \beta_j F_{t-j} + \sum_{k=1}^{K} b_k \tilde{h}_{t-k} + H_t^{1/2} e_t \tag{2}$$

$$\tilde{h}_{t+1} = \alpha + \theta \tilde{h}_t + \sum_{j=1}^{Q} d_j F_{t-j} + S^{1/2} \eta_t \tag{3}$$

Here $\underbrace{X_t}_{n\times 1}$ denotes the cross-country panel of CPI inflation rates and industrial production growth. Our benchmark model includes CPI inflation data for 205 countries. We also include industrial production growth which is available for a subset of 52 countries. The vector $\underbrace{f_t}_{N_f\times 1}$ denotes the unobserved common factors and, as described below, $\underbrace{z_t}_{N_z\times 1}$ are observed factors used as additional predictors. The idiosyncratic components $\underbrace{\left(v_t\right)}_{n\times 1}$ are assumed to be serially correlated: $v_{it} = \sum_{l=1}^{L} \rho_i v_{it-l} + u_{it}$ for $i = 1, 2, \ldots, n$, where the disturbances u_{it} have a diagonal variance-covariance matrix: $u_t \sim N(0, R_t)$ where $R_t = diag\left(\exp\left(\tilde{r}_t\right)\right)$ with $\tilde{r}_t = [r_{1t}, r_{2t}, \ldots, r_{n,t}]$. Each of these volatilities are assumed to evolve as random walks.

The factors $\underbrace{F_t}_{N\times 1} = \begin{pmatrix} z_t \\ f_t \end{pmatrix}$ VAR model with stochastic volatility in equation 2. The stochastic volatilities are denoted by $\tilde{h}_t = [h_{1t}, h_{2t}, \ldots, h_{N,t}]$ and $H_t = diag\left(\exp\left(\tilde{h}_t\right)\right)$. As evident, $\tilde{h}_t$ is allowed to have a lagged impact on the factors. The stochastic volatilities evolve according to equation 3. The shocks to this equation have a variance $S = diag(\tilde{s})$ with $\tilde{s} = [s_1, s_2, \ldots, s_N]$. Note that θ can be a full matrix with the elements of $\tilde{h}_t$ allowed to have a dynamic relationship amongst themselves.

The disturbances $\varepsilon_t = \begin{pmatrix} \eta_t \\ e_t \end{pmatrix}$ are distributed normally $N(0, \Sigma)$ where the diagonal elements of Σ are restricted to equal 1:

$$\Sigma = \begin{pmatrix} \Sigma_\eta & \Sigma'_{\eta_t e_t} \\ \Sigma_{\eta_t e_t} & \Sigma_{e_t} \end{pmatrix} \tag{4}$$

In other words, the time-varying covariance matrix of the reduced form residuals of the system in equations 1 and 2 can be written as:

$$\Omega_t = \begin{pmatrix} S^{1/2} & 0 \\ 0 & H_t^{1/2} \end{pmatrix} \begin{pmatrix} \Sigma_\eta & \Sigma'_{\eta_t e_t} \\ \Sigma_{\eta_t e_t} & \Sigma_{e_t} \end{pmatrix} \begin{pmatrix} S^{1/2} & 0 \\ 0 & H_t^{1/2} \end{pmatrix}' \tag{5}$$

Thus, the model allows for correlation between the shocks to the level of the factors and volatilities.

The proposed Dynamic Factor Model (DFM) offers significant advantages over alternative approaches like panel quantile regressions (for example, Furceri et al., 2025). Notably, the DFM inherently captures cross-country relationships through common factors and conveniently accommodates mixed frequency and unbalanced panel data. This provides a robust method for estimating the response of risk measures to structural shocks. Furthermore, Caldara et al. (2024) demonstrate that the DFM's density forecasting performance is comparable to quantile regressions, delivering well-calibrated forecast distributions for real activity and inflation.

2.2 Missing values and mixed frequency data

Unlike Caldara et al. (2024), we work with a panel of data X_t that features a mix of monthly and quarterly inflation rates and also includes series where data is missing at the beginning of the sample.[3] Following Marcellino et al. (2016), we formulate the measurement equation 1 in terms of observed data. For series that are available at a quarterly frequency (over part or all of the sample), we assume the following relationship to monthly data:

$$\hat{X}_{it} = B_f f_t + B_z z_t + \hat{v}_t \tag{6}$$

where $\hat{X}_{it}$ denotes the latent monthly data. The observed data at the quarterly frequency X_{it}^{Q} are assumed to be an average of the monthly data that are treated as latent variables. For the quarters where data is available, X_{it}^{Q} is related to $\hat{X}_{it}$ through:

$$X_{it}^{Q} = \frac{1}{3}\sum_{j=0}^{2} \hat{X}_{it-j} \tag{7}$$

where we assume that X_{it}^{Q} is observed in the last month of the quarter. Substituting equation 7 into equation 6 we obtain the observation equation:

$$X_{it}^{Y} = \frac{B_f}{3}\left(\sum_{j=0}^{2} f_{t-j}\right) + \frac{B_z}{3}\left(\sum_{j=0}^{2} z_{t-j}\right) + \frac{1}{3}\sum_{j=0}^{2} \hat{v}_{it-j} \tag{8}$$

Therefore, when data are available for the quarterly series assigned to the third month of the quarter, the observation equation is given by equation 7. In contrast, when observation is missing (for quarterly or monthly series) the observation equation is defined as:

$$X_{it}^{-Q} = u_{it}, var\left(u_{it}\right) = 1e10 \tag{9}$$

with the large error variance ensuring that the observation is skipped in the Kalman filter. Finally, when monthly data is available, then the observation equation is given by equation 1.

[3] Most series in the panel are available at a monthly frequency. However, a subset of inflation rates are only available quarterly. See section 3 for more details.

2.3 Observed factors z_t

As noted above, we incorporate the observed factors z_t as predictors. These factors are estimated as K principal components from a large unbalanced cross-country dataset of variables $\underbrace{z_t}_{843\times1}$ that potentially contain relevant information for predicting CPI inflation. This panel includes data on food and energy CPI inflation, 3 month treasury bill rates, growth of nominal effective exchange rates and commodity price indices where available for the 205 countries we consider. We estimate these factors using the principal component estimator described in Stock and Watson (2002). The Expectation-Maximization (EM) algorithm proposed by Stock and Watson (2002) allows us to include countries in this monthly panel where the data features missing values or the time-series are only available at quarterly frequencies.

While it is theoretically possible to merge z_t and X_t and treat missing values and mixed frequencies in the state-space framework described in equations 8 and 9, the large cross-section dimension and the large proportion of series with missing values makes this computationally infeasible. This is because out of the 843 series in Z_t, 86 percent contain missing values. In the state-space framework, this implies more than 600 additional latent states making forward and backward filtering prohibitively slow.

2.4 Gibbs sampling algorithm

We use an MCMC algorithm that is partly based on the procedure described in Caldara et al. (2024) and Mumtaz (2018). As we describe below, the key difference in our approach is that we allow for mixed frequency and unbalanced data when sampling from the conditional posterior of the factor loadings and the factors. We provide a sketch of the algorithm in this section with details confined to the appendix. The algorithm samples from the following conditional posterior distributions:

1. Factors f_t: Conditional on z_t, the remaining parameters and stochastic volatilities, the measurement equation is given by 1 when no missing observations are present in the series. However, for series that are available at the quarterly frequency, the measurement equation is given by 8 when the data are observed at the end of each quarter. Note that the idiosyncratic components for these series are treated as latent states. when observations are missing, the measurement equation 9 is used. The transition equations are given by the VAR in 2 and the AR for the idiosyncratic components. This state-space model is conditionally linear and Gaussian and we draw f_t using the Carter and Kohn (1994) algorithm.

2. Factor loadings $B = \begin{pmatrix} B_f \\ B_z \end{pmatrix}$: Given the factors F_t and the volatilities r_{it}, the factor loadings are coefficients in $i = 1, \ldots n$ linear regressions with a known form of heteroscedasticity. When the corresponding dependent variable X_{it} does not contain missing values and is available at a monthly frequency, the conditional posterior distribution is normal after a GLS transformation of the data and standard methods for Bayesian Linear regressions apply. However, when X_{it} has missing values, the conditional posterior is non-standard as the underlying monthly data is treated as latent. In this case, we use a Metropolis Hastings step to draw the factor loadings.

3. Persistence of idiosyncratic shocks ρ: Conditional on the idiosyncratic shocks, the AR coefficients ρ_i can be easily drawn using methods for linear regressions applied to each residual v_{it} for $i = 1, \ldots, n$

4. Volatility r_{it}: Conditional on the factors, factor loadings, the observation equation is a set of n independent univariate stochastic volatility models. We draw the volatilities from their conditional posterior using the algorithm of Jacquier et al. (2002). The variances g_i have a Inverse Gamma (IG) conditional posterior and can be easily simulated.

5. Coefficients of the transition equation B: The conditional posterior distribution of the coefficients $B = vec\left([\alpha, \theta, d_1, .., d_Q, c, \beta_1, .., \beta_P, b_1, .., b_K]\right)$ can be obtained by writing equations 1 and 2 as a seemingly unrelated regression system. Given $\tilde{h}_t$, the disturbances of the system are normal with covariance matrix Σ. With a normal prior, the conditional posterior of $\mathcal{B}$ is also normal. The Kalman filter can be used to find the mean and variance of the conditional posterior taking into account the time-variation in H_t.

6. Variance of the shocks to volatility S: The correlation among the disturbances of the transition equation $\tilde{\eta}_t = S^{1/2}\eta_t$ implies that the conditional posterior for the elements of S is non-standard and a Metropolis step is required. A candidate density that displays satisfactory performance in simulations is the IG distribution centered at the posterior moments calculated under the assumption that $\tilde{\eta}_t$ are uncorrelated, i.e. $IG\left(v_1, T_1\right)$, $v_1 = \tilde{\eta}_{it}'\tilde{\eta}_{it} + v_0$ and $T_1 = T_0 + T$ where v_0, T_0 denote prior moments and T is the sample size. In practice, this can also be combined with a IG distribution centered on the previous draw to obtain a mixture proposal density. Note that given $F_t, \mathcal{B}, \Sigma, \tilde{h}_t$ and a draw of S from the candidate density, the likelihood can be easily calculated with the process described in the appendix.

7. Correlation matrix of the residuals Σ: Given B and the variances $S, \tilde{h}_t$, the residuals ε_t. The draw of the restricted covariance matrix is obtained via the independence Metropolis algorithm described in Chan and Jeliazkov (2009).

8. Stochastic Volatility $\tilde{h}_t$: Conditional on the remaining parameters, the observation equation of the state-space system can be written as:

$$\begin{aligned} F_t - H_t^{1/2}\mu_{e_t|\eta_t} &= c + \sum_{j=1}^{P}\beta_j F_{t-j} + \sum_{k=1}^{K} b_k \tilde{h}_{t-k} + \tilde{e}_t \\ var\left(\tilde{e}_t\right) &= \Omega_t = H_t^{1/2}\Sigma_{e_t|\eta_t} H_t^{1/2\prime} \end{aligned}$$

where $\mu_{e_t|\eta_t}$ denotes the conditional mean of e_t and $\Sigma_{e_t|\eta_t}$ is the conditional variance:

$$\begin{aligned} \mu_{e_t|\eta_t} &= \eta_t \Sigma_{\eta_t}^{-1}\Sigma_{\eta_t e_t}' \\ \Sigma_{e_t|\eta_t} &= \Sigma_{e_t} - \Sigma_{\eta_t e_t}\Sigma_{\eta_t}^{-1}\Sigma_{\eta_t e_t}' \end{aligned}$$

We treat η_t as a state variable in this step and write the transition equation as

$$\digamma_t = C + \Psi \digamma_{t-1} + N_t$$

where $\digamma_t = \begin{pmatrix} \eta_{t+1} \\ \eta_t \\ \tilde{h}_{t+1} \\ \vdots \\ \tilde{h}_{t-k} \end{pmatrix}$. Note that the residual of the transformed observation equation $\tilde{e}_t$ is uncorrelated with N_t. As described in the appendix, we employ a particle Gibbs step (see Andrieu et al. (2010) and Lindsten et al. (2014)) to sample $\digamma_t$ from its conditional posterior distribution.

2.5 Model specification and predictive distributions

We estimate the model using $N_f = 3$ unobserved factors that explain about 60 percent of the variation in the panel of CPI inflation rates and industrial production growth X_t. We also include $N_z = 5$ observed factors that capture the bulk of the information in Z_t. The lag length P and K in equation 2 is set to 6 and 1 respectively. We use 1 lag of the factors in the transition equation for volatility in equation 3. Finally the idiosyncratic components follow an AR(1) process. We show in the robustness checks that altering the number of factors and lags does not materially change the main results. The MCMC algorithm described above uses $11,000$ iterations with a burn-in of 1000, with every 10^{th} draw retained. We use the posterior draws to calculate the posterior predictive density $p(X_{it+h}|X_{it}, F_T, H_t, R_{it}, \Theta)$ where Θ denotes all fixed parameters. Note that this density takes into account parameter and latent state uncertainty, along with future uncertainty regarding shocks, and the volatility associated with the factors and idiosyncratic components. We consider the forecast distribution at the one year horizon in the analysis below.

3 The Data

The analysis is based on a large cross-country panel spanning January 1971 to December 2023. The core dataset, denoted X_t, comprises headline consumer price index (CPI) inflation and industrial production (IP) growth, expressed as annual growth rates. The panel covers 205 economies.

CPI inflation data are available for all countries in the sample. Industrial production data are available for a smaller subset of 52 economies, primarily advanced economies and large emerging markets. As summarized in Table A.1, the dataset is highly unbalanced: approximately 80 percent of the series contain at least one missing observation, and 19 countries report CPI inflation only at a quarterly frequency over part or all of the sample period. CPI inflation data are drawn from the World Bank Global Inflation Database compiled by Ha et al. (2019). Industrial production data are obtained from Haver Analytics. All series are transformed into year-on-year growth rates to ensure comparability across countries and to focus on medium-term inflation dynamics.

In addition to the core variables explained above, as noted in Section 2, the model incorporates a set of observed predictors, denoted z_t, which are constructed from an auxiliary panel Z_t of country-level time series. This panel includes, where available, food and energy CPI inflation, short-term interest rates, growth in nominal effective exchange rates, and commodity price inflation. These variables are chosen to capture key global and domestic drivers of inflation dynamics. The auxiliary panel Z_t is unbalanced and features substantial variation in data availability across countries and over time. The construction of the observed factors z_t and their role in the econometric framework are described in Section 2.

Taken together, the data exhibit three salient features: broad cross-country coverage, pervasive missing observations, and mixed-frequency reporting. These characteristics motivate the econometric framework developed in the preceding section.

4 Results

4.1 Global inflation risk

We use the model to compute the one-year-ahead predictive density for a weighted average of CPI inflation rates on an annual basis across our panel using purchasing power parity (PPP) GDP weights. This object is constructed using as initial conditions the data and estimated states at each point in the sample to obtain the predictive density.

Figure 1 shows how the tails of the predictive density evolve over time. It is interesting to note that the density is skewed to the right over most of the sample. The mid-1970s and the early and mid-1980s are the only periods where there is substantial mass below zero, reflecting high and volatile inflation during the period (figure 1A). After the mid-1990s, the forecast distribution narrows substantially, consistent with the prolonged period of low and stable inflation. Beginning in 2020, however, the predictive distribution shifts markedly to the right, with both the median forecast and the upper tail increasing sharply during the COVID-19 pandemic (figure 1B).

Figure 1: The forecast distribution for Global CPI inflation

A. Entire sample

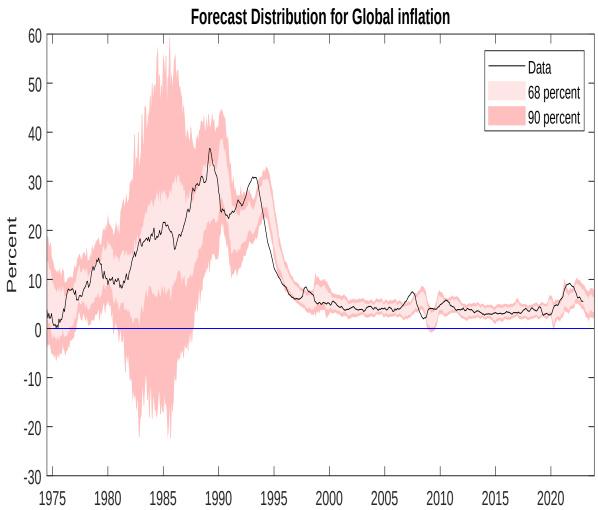

B. Post 2010

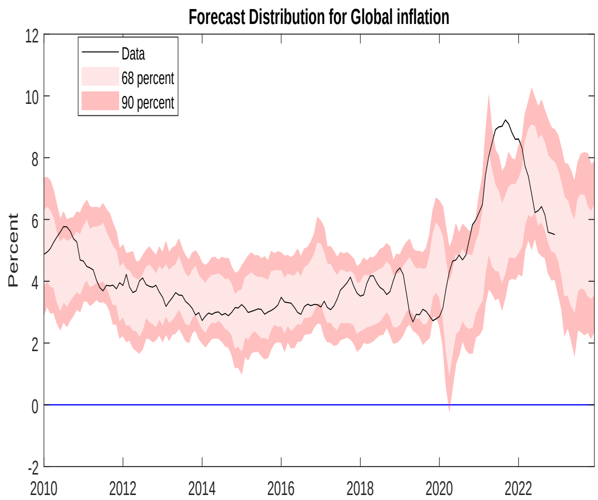

Source: Authors' calculations.
Note: Global inflation is a weighted average of CPI inflation rates for each country using PPP GDP weights. The figure shows the one year ahead forecast distribution obtained at each point in the sample. The solid line is the realised Global inflation rate one year ahead.

We summarize these distributional shifts using our benchmark measure of inflation risk: the probability that global CPI inflation twelve months ahead exceeds 5 percent. Figure 2 plots this estimated risk measure for global inflation. The initial period, stretching from 1975 through the late 1990s, reveals a consistently high probability of global inflation surpassing 5 percent, often exceeding 80 percent and hitting peaks near 100 percent during the late 1970s and early 1980s. This aligns with the historical Great Inflation era, characterized by oil shocks and expansionary monetary policies. An elevated risk is also observed in the mid-1990s, coinciding with world inflation rates reaching over 9% in 1995.

Figure 2: The probability that global inflation will exceed 5 percent one-year ahead

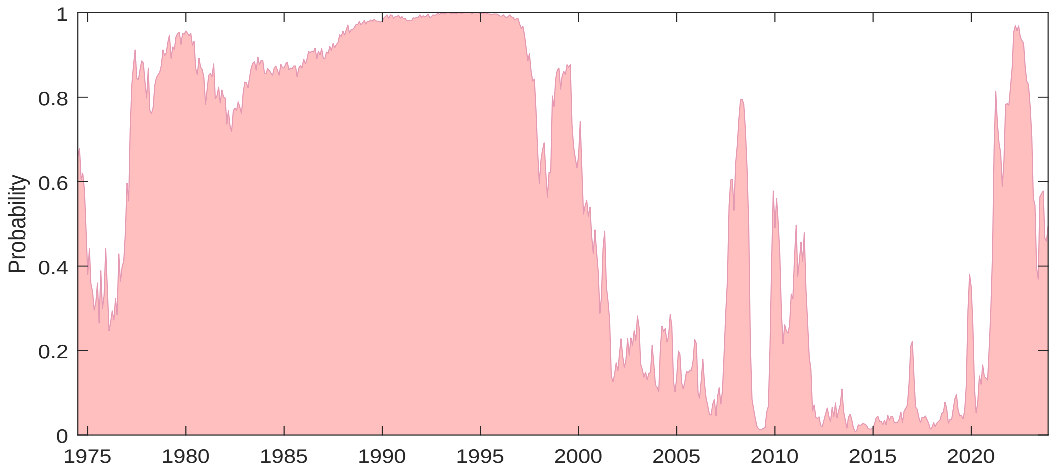

Note: The probability that global inflation will exceed 5 percent one-year ahead. This is computed using the forecast distribution shown in Figure 1.

Following a sharp decline around 1998-2000, the measure of inflation risk declined, largely reflecting the Great Moderation. During much of the 2000s and 2010s, the probability generally remained below 20%. However, temporary increases in risk are discernible around 2008-2009, likely reflecting the global financial crisis and associated commodity price volatility, and a smaller spike in the early 2010s. Towards the very end of the depicted period, around 2020, the probability exhibits a dramatic and rapid increase, surging back towards levels not witnessed since the late 1990s. This sharp rise anticipates the global inflation surge experienced following the COVID-19 pandemic and subsequent supply chain disruptions and geopolitical events, where global inflation rates indeed rose sharply.

4.2 Cross-country heterogeneity

Figure 3 presents our estimated risk measure for six major world regions. While regional inflation risk generally co-moves with the global measure, substantial heterogeneity is evident. The estimated risk in North America and Oceania track global patterns with values close to 1 prior to the early 1990s, followed by a sustained decline in the pre-Covid period and a sharp rise after 2020. In Europe, inflation risk rose after the mid-1980s and remained elevated until the early 2000s. European countries also saw a sharp rise in inflation risk at the end of the sample. The estimated risk follows a similar temporal pattern in Asia, albeit with the distinguishing feature that risk was elevated in the aftermath of the Great Financial crisis in 2009/2010. African and South-American countries appear to be different from the remaining sample, with the risk measure persistently high throughout the sample.

Figure 3: The probability that regional inflation will exceed 5 percent one-year ahead

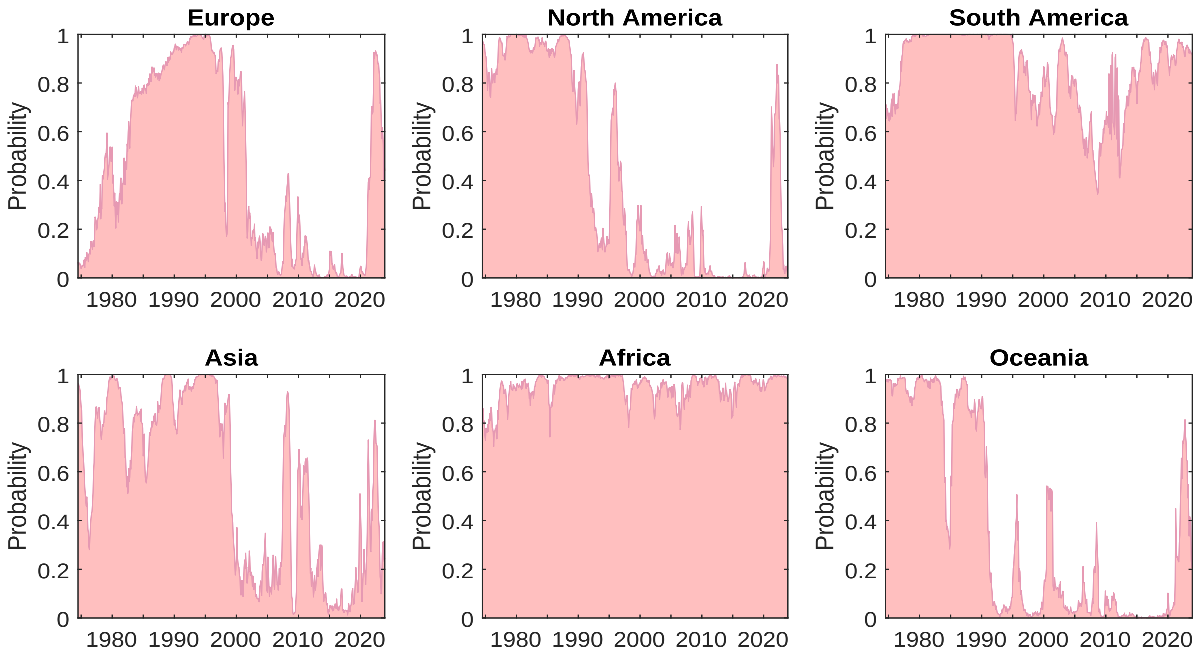

Note: The probability that Regional inflation will exceed 5% one year ahead. This is computed using the forecast distribution of PPP GDP weighted regional inflation rates.

While these cross-regional differences broadly reflect regionally clustered country-specific characteristics, they appear to mask substantial heterogeneity at the country level as well. Figure 4 maps the average probability that inflation exceeds 5 percent across countries over the sample period and highlights pronounced geographic clustering in inflation risk. Elevated risk is concentrated in parts of South America, Africa, Eastern

Europe, and Central Asia, where inflation has historically been more volatile and episodes of high inflation more frequent. By contrast, much lower inflation risk is observed across most advanced economies, including North America, Western Europe, and parts of East Asia.

The spatial distribution of inflation risk in Figure 4 suggests that persistent differences in policy frameworks and structural characteristics may have played an important role in shaping inflation tail outcomes. The extensive literature establishes that countries with historically higher inflation risk tend to be those with weaker monetary institutions, greater exposure to commodity price fluctuations, or more limited integration into global trade and financial markets (Ha et al., 2019). These patterns motivate the analysis in Section 6, which formally examines the relationship between inflation risk and country-specific structural and policy characteristics.

Figure 4: The probability that consumer inflation will exceed 5 percent one-year ahead

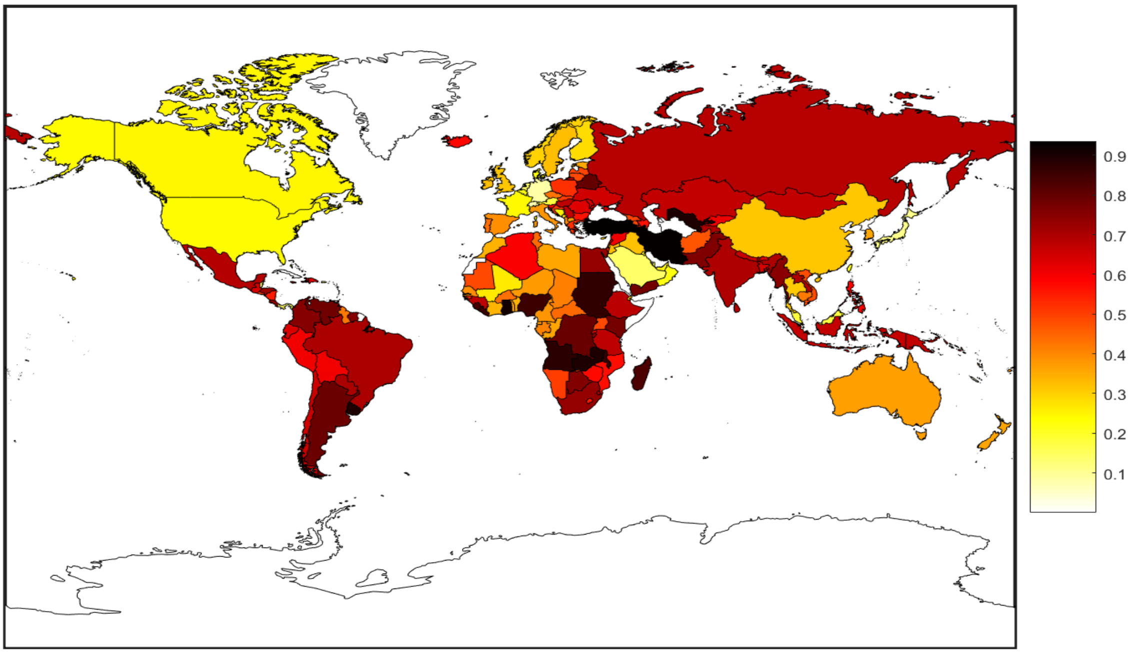

Note: The probability that inflation will exceed 5% one year ahead. Average across sample dates. Darker shades indicate higher risk. White colour indicates unavailability of data for that country. The boundaries and other information shown on this map do not imply any judgment concerning the legal status of any territory or the endorsement or acceptance of such boundaries.

4.3 Risk of stagflation

An important advantage of the dynamic factor model is that it allows us to characterize the joint predictive distribution of inflation and real activity. This feature enables the analysis of stagflation risk, defined as the probability that inflation exceeds 5 percent one year ahead while industrial production (IP) growth is negative at the same forecast horizon. We compute this joint probability for the 51 countries for which both CPI inflation and IP data are available over the sample period. As in the previous sections, the probabilities are obtained from the one-year-ahead predictive distributions implied by the estimated model, taking into account uncertainty from shocks, stochastic volatility, and parameter estimation.

Figure 5 plots the evolution of global stagflation risk, constructed as a PPP GDP–weighted average across the 51 countries for which both inflation and industrial production data are available, alongside the corresponding measure of global inflation risk. Two features stand out. First, stagflation risk was elevated during the late 1980s and early 1990s, reflecting a period in which high inflation coincided with weak real activity in several major economies. Following this episode, stagflation risk declined steadily and remained low throughout much of the 2000s and 2010s, even during periods when inflation risk was non-negligible.

Figure 5: Stagflation risk

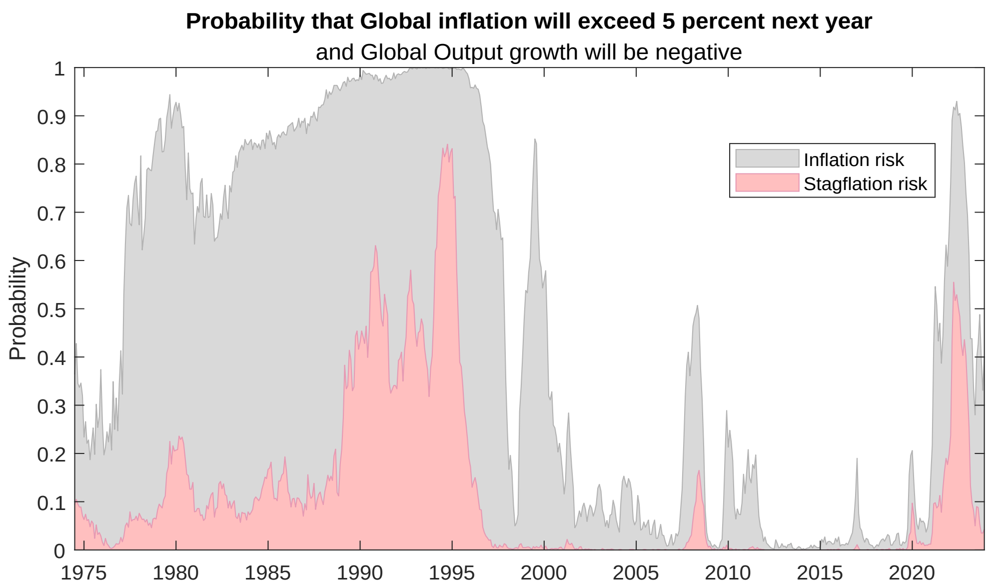

Note: The probability that Global inflation will exceed 5% one year ahead and Global IP growth will be negative at that horizon (pink shaded area). This is compared with Global inflation risk in these 51 countries (grey shaded area).

Second, the COVID-19 episode marks a sharp but short-lived departure from this pattern. In October 2021, the estimated probability of global stagflation briefly exceeded

50 percent, driven by the simultaneous surge in inflation risk and the contraction in real activity across a broad set of countries. As Figure 5 makes clear, however, stagflation risk declined rapidly thereafter as output recovered, despite inflation risk remaining elevated. The divergence between inflation risk and stagflation risk during this period underscores the importance of accounting for the joint distribution of inflation and real activity, rather than assessing inflation risks in isolation.

Figure 6: Probability of stagflation

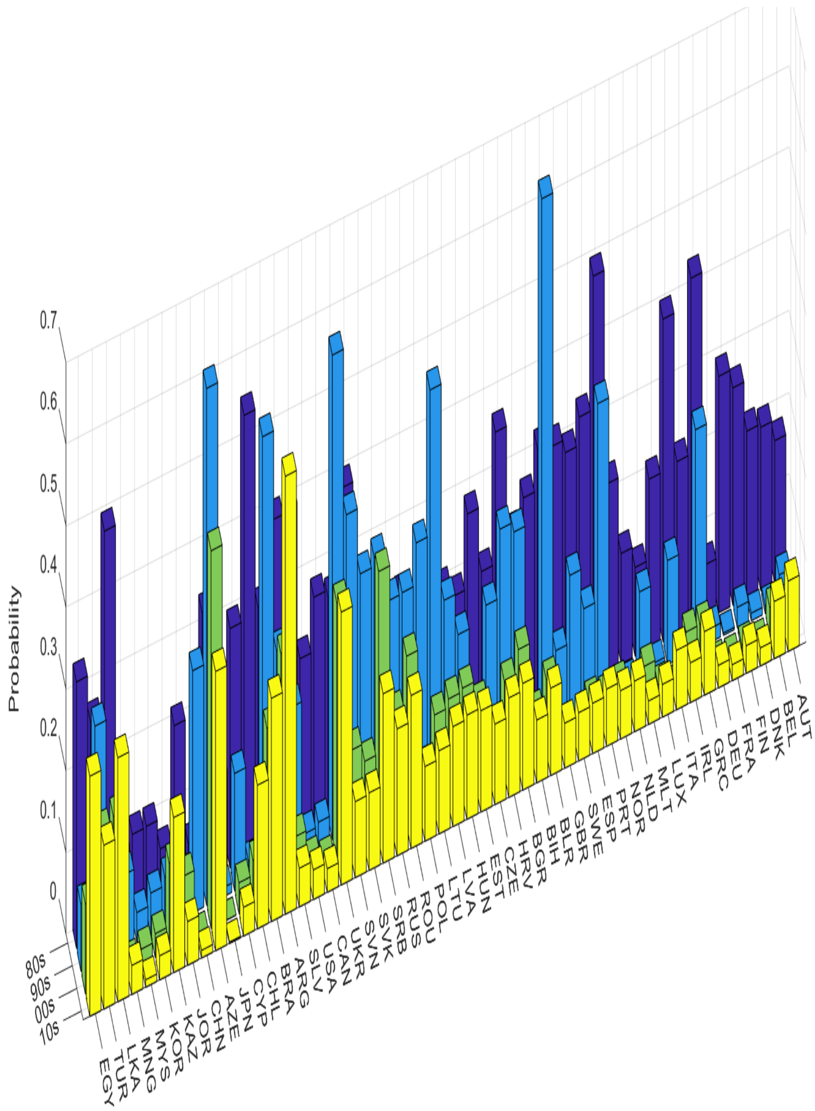

Note: The probability that global inflation will exceed 5% one year ahead and global IP growth will be negative at that horizon. Average is shown before 1990 (80s), between 1990 and 2000 (90s), between 2000 and 2010 (00s) and after 2010 (10s).

Figure 6 then highlights substantial heterogeneity in stagflation risk across countries and over time. Averaged over the sample, stagflation risk is markedly higher in emerging market economies such as Argentina, Azerbaijan, Brazil, and Ukraine, reflecting repeated episodes in which elevated inflation coincided with weak or volatile real activity. In contrast, advanced economies—including Germany, Japan, Malaysia, and South Korea—exhibit consistently lower average stagflation risk, consistent with more stable inflation dynamics and stronger real activity performance.

The timing of stagflation risk also differs systematically across countries. For most economies, the probability of stagflation is highest prior to or during the 1990s, in line with the global disinflation that followed this period. More recent episodes of elevated stagflation risk are comparatively rare and tend to be short-lived, even in countries experiencing high inflation. These patterns suggest that while stagflation risk remains an important vulnerability in some economies, it is highly episodic and closely linked to country-specific structural features and policy frameworks. This heterogeneity motivates the analysis in the next section, which examines how national characteristics help explain differences in inflation risk across countries.

Overall, these findings suggest that stagflation risk is highly episodic and varies substantially across countries and over time. While global stagflation risk rose sharply during the pandemic, such episodes are relatively rare and depend critically on the joint behavior of inflation and real activity. The results underscore the value of joint density-based measures for assessing macroeconomic vulnerabilities that are not captured by single-variable risk indicators.

5 Inflation risk, shocks, and monetary policy

The previous section documents pronounced time variation and cross-country heterogeneity in inflation risk. To shed further light on the sources of these differences, this section examines the cyclical determinants of inflation risk, focusing on the role of macroeconomic shocks and monetary policy.

5.1 Macroeconomic shocks and inflation risk

We consider how inflation risk responds to demand and supply type disturbances. We follow Caldara et al. (2024) and Koop et al. (1996) and compute the response of our risk measure for each country by simulation. In particular we generate a counterfactual forecast distribution for inflation for each country. This is done by computing a conditional forecast for each iteration of the Gibbs algorithm using initial conditions at time t and assuming that the system is subject to a shock of interest in the first period of the simulation. This is repeated J times and the average of the projected data delivers the forecast conditional on a shock for Gibbs iteration i. Repeating this for Gibbs iterations $i = 1, 2, \ldots, I$ delivers a counterfactual distribution for the forecast of inflation. We compute the impulse response as probability of inflation next year exceeding 5 percent implied by this counterfactual distribution minus the same probability obtained using the forecast distribution that is computed under the assumption of no additional shocks.

We consider two basic structural shocks that are identified via sign restrictions. We assume that the demand shock moves average IP growth, average CPI, food and energy inflation, in the same direction.[4] This shock captures disturbances associated with global business cycle. The supply shock is identified via the assumption that it moves average IP growth and the inflation measures noted above in opposite directions. The sign restrictions are imposed on the contemporaneous period and 2 months after the shock and impulse response of the panel variables are computed via simulation as in Koop et al. (1996).[5] Figure A.3 in the appendix shows the response of average real activity and inflation measures to this shock. As shown in the figure, the two shocks are calibrated to increase CPI inflation by about one percent on impact.

Figure 7 reports the impulse responses of inflation risk to these shocks across six major world regions. For each region, the solid line denotes the median response across countries, while the shaded area represents the 5th and 95th percentiles. Several patterns emerge. First, both demand and supply shocks lead to increases in inflation risk across all regions, reflecting the nonlinear nature of the predictive distribution. Second, supply shocks tend to generate larger median increases in inflation risk than demand shocks in Europe, Africa, and Oceania. In other regions, the distributions of country-level responses overlap more closely across shock types.

To assess the relative importance of these disturbances in driving inflation risk over longer horizons, Figure 8 presents the contribution of demand and supply shocks to the forecast error variance (FEV) of inflation risk at the two-year horizon.[6] In most regions, demand shocks account for a larger share of the variance in inflation risk than supply shocks, as reflected in higher median contributions across countries. Europe stands out as an exception, where supply shocks exhibit a wider dispersion and account for a substantial share of inflation risk for countries in the upper tail of the distribution.

Overall, these results suggest that both demand and supply shocks play important roles

[4]We consider weighted averages when imposing restrictions with PPP GDP shares used as weights.
[5]The number of Monte-Carlo replications J is set to 50.
[6]The contributions are calculated using the methods described in Lanne and Nyberg (2016).

Figure 7: Impulse response of inflation risk

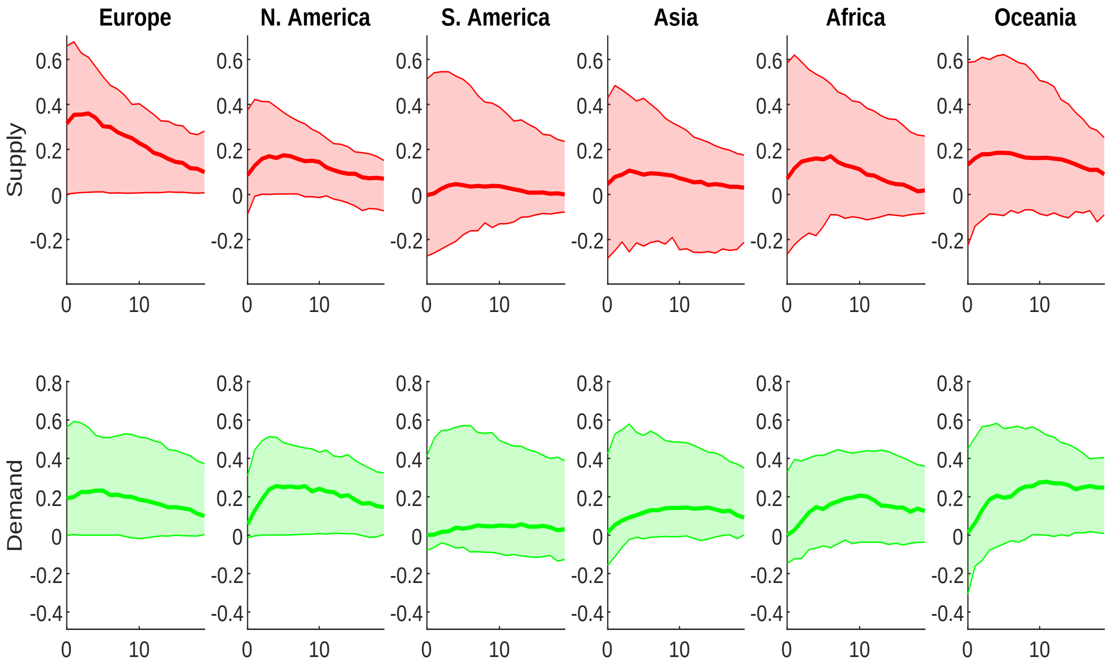

Note: Impulse response of the probability that regional inflation will exceed 5% one year ahead. The shaded area represents the 5th and 95th percentile of the response of countries in the region.

in shaping inflation tail risks, but their relative importance varies across regions. Notably, supply shocks appear to be particularly relevant for explaining episodes of heightened inflation risk in Europe, highlighting the sensitivity of inflation tail outcomes to adverse supply conditions.

5.2 Monetary policy cycles and inflation risk

Periods of monetary policy tightening offer a natural setting to study the relationship between central bank actions and inflation risk. When central banks embark on hiking cycles–in response to elevated or persistent inflation–they aim not only to reduce realized inflation but also to anchor expectations and mitigate the probability of future inflation overshoots. Using an approach similar to Forbes et al. (2024), we identify distinct phases of monetary policy cycles using policy rate data for 97 economies from January 1970 to January 2025.

We then examine how inflation risk evolves at the onset of monetary policy tightening cycles using an event-study framework. For each country, the start of a hiking cycle is

Figure 8: Contribution to inflation risk

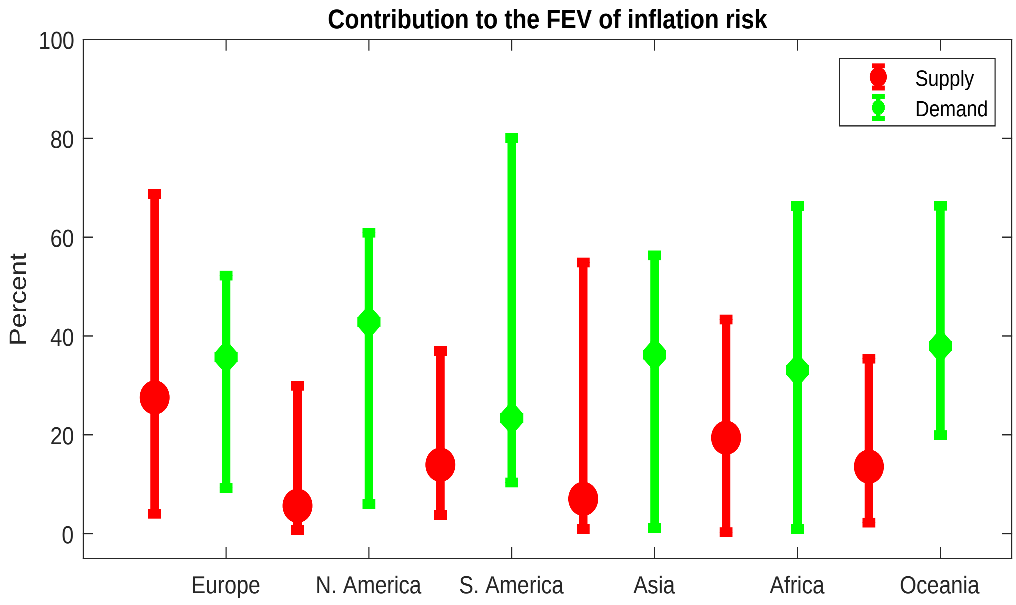

Note: Contribution to the FEV of the probability that regional inflation will exceed 5% one year ahead. The error bars represent the 5th and 95th percentile of the response of countries in the region while the dot is the median.

defined as the first month of a sustained period in which policy rates rise. To avoid overlapping events, hiking-cycle starts are required to be separated by at least 36 months. For every event, we construct a balanced event window spanning 12 months before and 24 months after the start of the hiking cycle. The dependent variable is the level of inflation risk relative to the month immediately preceding the hiking cycle ($\tau = -1$). The model includes event and time fixed effects.[7] We include interaction terms to distinguish between responses in EMDEs and advanced economies.

Following the start of a hiking cycle, inflation risk initially changes little, but after approximately one year there is evidence of a decline in inflation risk. Beginning around month 13, the coefficients become statistically significant and continue to fall over the subsequent year. By 20–24 months after the start of a hiking cycle, inflation risk is between 4 and 5 percentage points lower than in the month immediately preceding the first rate increase. The delayed response is consistent with the well-known lags in monetary transmission, suggesting that tightening cycles gradually reduce the probability of future inflation overshoots rather than generating an immediate improvement in inflation risk.

The event-study estimates provide little evidence of pre-existing trends in inflation

[7]Standard errors are clustered at the country level.

risk prior to the start of hiking cycles. In the twelve months before the first rate increase, inflation risk does not vary much with a joint test of the pre-treatment coefficients not significantly different from zero. This supports the identification assumption that inflation risk was not already declining before monetary tightening began.

There are differences between advanced economies and EMDEs, with the latter group driving the reduction in inflation risk after the start of a hiking cycle (figure 9). The weaker response in EMDEs is consistent with the notion that monetary transmission may be less effective where inflation expectations are less firmly anchored, policy transmission is weaker, policy credibility is lower, or exchange rate and supply-side shocks play a larger role in driving inflation dynamics.

Figure 9: Inflation risk around hiking cycles

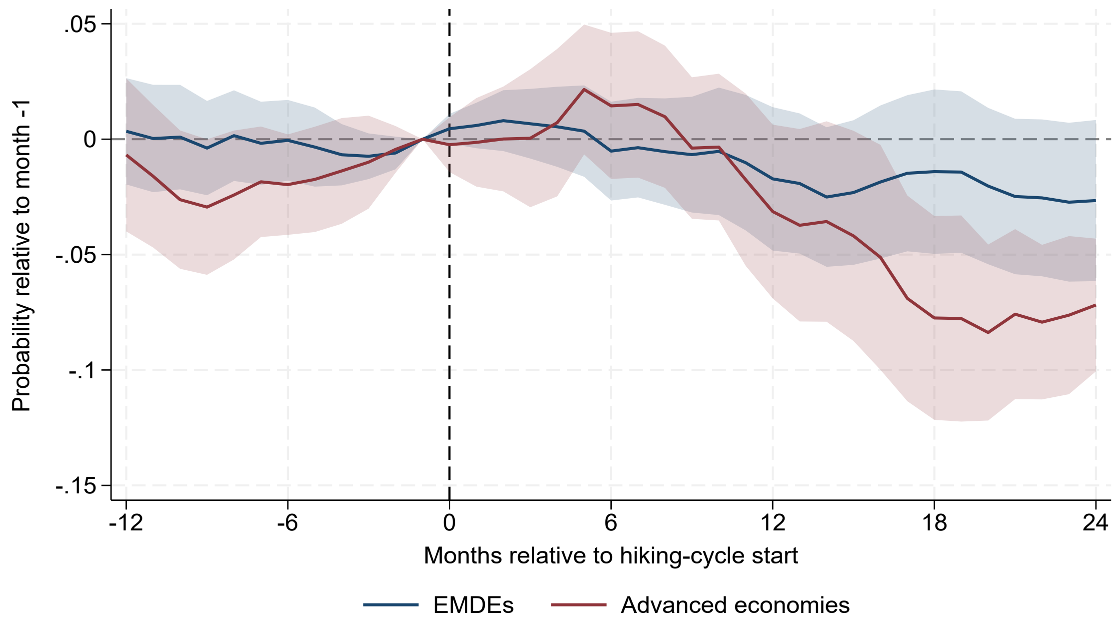

Note: The figure reports event-study estimates of inflation risk around the start of monetary policy hiking cycles for advanced economies and emerging market and developing economies (EMDEs). Event time is measured in months relative to the first month of a hiking cycle, with the month immediately preceding the cycle omitted as the reference period. Coefficients are estimated from a stacked event-study specification including event fixed effects and time fixed effects. Shaded areas denote 95 percent confidence intervals based on standard errors clustered at the country level. Hiking-cycle starts are required to be separated by at least 36 months, and the estimation window spans 12 months before and 24 months after each event.

6 Inflation risk and country characteristics

Section 4 identified substantial regional and cross-country variations in inflation risk. In this section, we examine various slow-moving national characteristics that help explain how inflation risk evolves over time. We employ multiple estimation techniques to capture the heterogeneous effects across countries and to analyze the behavior of inflation risk across several decades. As summarized in the previous section, a number of structural changes and long-term global trends have influenced inflation risk (and the process of inflation). Our analysis concentrates on two broad categories of country-specific characteristics: those related to the monetary policy framework and those linked to structural economic factors. The first category includes variables such as central bank independence, adoption of inflation targeting, and the exchange rate regime. The second encompasses trade openness, commodity-exporting status, and financial openness.

To investigate the relationship between these characteristics and inflation risk, we use both descriptive statistics and regression analysis, situating our findings within the context of the existing literature. We also conduct a series of group mean difference tests to examine variations in inflation risk across country groups over fixed forecasting horizons from the 1970s through the 2010s. Our sample covers 122–192 countries, depending on data availability for inflation-related variables, of which 118–147 are emerging market and developing economies (EMDEs).

In the regression analysis, inflation risk is modeled as $\Delta\pi_{it} = \alpha + \beta X_{it}$, with robust standard errors. Here, $\Delta\pi_{it}$ represents the country-specific change in inflation risk over time t, and X_{it} denotes the relevant country characteristics. Changes in inflation risk are calculated as differences in averages between 1974–79 and 2010–19. The intercept α captures the unconditional average decline in inflation risk over this period. Given the high correlation among many explanatory variables, we estimate bivariate regressions to avoid multicollinearity. The regressors X_{it} include: changes in trade openness (measured as trade as a percentage of GDP), changes in capital account openness (based on the Chinn-Ito index), adoption of an inflation targeting regime, adoption of a pegged exchange rate regime (as defined by Shambaugh, 2004), changes in central bank independence and transparency (measured using the Dincer and Eichengreen, 2014), and the share of commodity exports in GDP. These country characteristics used in this section are summarized in Table A.2.

The discussion that follows explores the relation between inflation risk and each of these country characteristics in greater detail.

6.1 Trade Openness

Increased openness to international trade is typically accompanied by higher shares of imports in consumption and production and lower prices (compared with a closed economy), owing to competitive pressures from foreign producers. It may also account for greater co-movement of inflation and it's volatility with the global measures.

Based on our analysis, countries that are more open to trade experienced lower inflation risk, than those with lower trade openness in most years (Figure 10A). This is consistent with the findings in the broad literature (including Bowdler and Malik, 2005 and Granato et al., 2006). The mean differences are significant, both economically and statistically, as $5^{th} - 95^{th}$ confidence intervals do not include zero, throughout the years between 1980 and 2022 (right chart of Panel A). The results from panel regressions (in Table A.3) lead to similar findings; in countries where trade openness increased more than others, by 10 percentage points of GDP over the past four decades, inflation risk declined by 0.01 percentage point more than average over the same period, which results hold using the EMDE sample only.[8]

6.2 Financial Openness

In theory, financial openness could raise or depress inflation volatility (Ha et al., 2019). If capital flows help smooth fluctuations in consumption in a financially open economy, they can moderate domestic demand swings that might otherwise generate inflationary or disinflationary pressures. This would reduce inflation volatility. Conversely, procyclical capital inflows could themselves generate larger domestic demand swings and cause greater volatility in output and inflation.

The descriptive statistics and the mean difference tests suggest that, beginning in the early 1990s, countries with greater capital account openness faced significantly lower inflation risk compared to those with more restricted capital accounts (Figure 10B). This trend persisted through the mid-1990s and beyond. Similarly, panel regression results indicate that a point increase in the capital account openness index over the past four decades was associated, on average globally, with 0.28 percentage point reduction in inflation risk and, among EMDEs, 0.07 percentage point reduction (though insignificant; see Table A.3).

[8]That said, advanced economies experienced the opposite, and a similar increase led to moderately higher (0.01 percentage point) inflation risk than those average over the same period. The positive relation in advanced economies may reflect endogeneity issues as higher trade-open developed economies tend to be associated with lower intrinsic inflation volatility than others.

6.3 Commodity Exporters

Commodity exporters exposed to volatile commodity prices could experience greater macroeconomic risk and volatility, including inflation risk. However, these could be moderate effects if these economies can fully stabilize output growth and exchange rate swings. Conversely, countries that rely heavily on food imports may be subject to greater global commodity price volatility. However, the consequences of resource reliance for macroeconomic stability may also depend on policy frameworks.

As shown in Figure 10C, the mean difference tests indicate that post-1990, inflation risk sharply declined for commodity importing countries compared to commodity-exporting countries (left chart). This difference has remained statistically significant throughout the years before the post-pandemic period partly reflecting the low level of energy prices compared with the 1970s and 1980s (right chart). The estimation results from the panel regressions in Table A.3 consistently suggest a positive relation between commodity exporting countries and inflation risk. The results for the regression with all countries (Panel A) suggest that commodity exporting countries have 0.17 percentage point higher inflation risk than non-commodity exporting countries (the coefficient is 0.13 for EMDEs).

6.4 Inflation Targeting framework

Increasing numbers of economies are adopting inflation targeting as their monetary policy framework, and this can help anchor expectations at the inflation target. This monetary policy regime can ensure that temporary shocks to inflation—caused, for example, by exchange rate swings or food price spikes—remain transitory and are not passed through to trend or core inflation.

Descriptive statistics provide some evidence of endogeneity between inflation targeting and inflation risk (or volatility). Prior to the 1990s, countries that adopted inflation targeting later exhibited significantly higher inflation risk compared to non-targeting countries (Figure 11A). However, this pattern fades and even reverses after 2010, although the difference is not statistically significant. These results suggest that countries—particularly EMDEs—that historically experienced high inflation volatility adopted inflation targeting and, subsequently, were able to effectively reduce inflation volatility.

The narratives on the importance of inflation targeting in reducing inflation risk is confirmed—particularly in advanced economies—by the panel regression. The results suggest that, over the past four decades, advanced economies that adopted an inflation targeting regime experienced a reduction of 0.28 percentage points in inflation risk (Table A.3B). As descriptive statistics suggested above, inflation risk has reduced for IT adopting

EMDEs, although not statistically significant, possibly due to the higher inflation risk in some EMDEs with IT in some regions (Latin America, South Asia, and Africa). These results are broadly consistent with the findings of Ardakani et al. (2018) and Stojanovikj and Petrevski (2021).

6.5 Exchange Rate Regime

A formal pegged exchange rate regime can signal a commitment to monetary and fiscal policy discipline, especially for those with weaker institutions. While pegged exchange rates can promote inflation stability and reduce volatility, sustained inflation differentials can undermine these benefits and ultimately lead to episodes of increased inflation volatility when the peg is tested or fails.[9]

The descriptive statistics and the mean difference test indicates that countries with pegged exchange rate regime had systematically lower inflation risk than those without pegged regimes (Figure 11 panel B). The regression results consistently lead to a negative relation between pegged exchange rate regimes and inflation risk. Economies with pegged exchange rate regimes, on average had 0.16 units less inflation risk over the four decades compared to those without pegged regime (Table A.3), and the relation is stronger for advanced economies. Ghosh et al. (1997) and Moreno (2001) also discuss similar findings.

6.6 Central Bank Independence and Transparency

A stability-focused monetary policy and exchange rate regime are reinforced by central bank independence and transparency. Greater independence enhances the central bank's credibility in achieving its policy goals, while increased transparency builds public trust, anchors inflation expectations, and fosters informed market and public discourse. Together, these qualities reinforce the effectiveness and legitimacy of monetary policy.

The results from the panel regressions in Table A.3 also indicate this as countries with high independence and transparency index have had 0.15 unit lower inflation risk over the decades compared to those with lower index (Dincer and Eichengreen, 2010 finds similar results). This is stronger for EMDEs and not statistically significant for advanced economies. In addition, as shown in Figure 11C, it is evident that since the 1990s, countries with greater central bank independence and transparency have experienced significantly smaller inflation risk compared to countries with less independent and less transparent

[9]If domestic inflation exceeds that of the anchor currency, pegging the exchange rate erodes competitiveness until inflation rates converge. Even after convergence, the loss in competitiveness can persist, creating pressures that may challenge the sustainability of the peg.

central banks. This effect has been statistically significant for most of the period since 1990.

7 Robustness Checks

This section assesses the robustness of the main findings along three dimensions: (i) alternative model specifications and estimation choices, (ii) sensitivity to the definition and construction of inflation risk, and (iii) robustness across empirical methodologies used to relate inflation risk to country characteristics. Detailed results are reported in appendix.

Model specification and estimation. We first examine the sensitivity of our results to alternative specifications of the dynamic factor model. As discussed in Section 2 and Appendix A1.2, we vary the number of latent factors, the lag structure in the factor VAR, and the dynamics of stochastic volatility. In particular, we consider models with additional latent factors and alternative lag lengths to assess whether the estimated inflation risk measures are driven by specific modeling choices. Across these specifications, the main qualitative patterns remain unchanged. The global measure of inflation risk continues to exhibit a pronounced decline during the Great Moderation and a sharp increase during the COVID-19 period. Similarly, the regional heterogeneity documented in Section 4 persists across alternative specifications. While the level of estimated inflation risk varies modestly with model complexity, the timing and relative magnitude of changes in inflation risk are highly stable.

Definition of inflation risk. A second set of robustness checks examines whether the main findings depend on the chosen threshold used to define inflation risk. While our baseline measure focuses on the probability that inflation exceeds 5 percent one year ahead, reports results using alternative thresholds and forecast horizons.[10] These exercises confirm that the key conclusions are not specific to the 5 percent cutoff. Periods identified as high-risk episodes under the baseline definition—most notably the late 1970s, early 1980s, and the post-2020 period—also correspond to elevated probabilities of extreme inflation under alternative definitions. Likewise, cross-country rankings of inflation risk are largely preserved, indicating that the measure captures broad tail-risk exposures rather than threshold-specific artifacts.

[10] Country-specific results are not reported in the paper, but a are available upon request.

Cross-country determinants: alternative empirical approaches. Finally, we assess robustness by exploiting the fact that Section 6 employs, by combining descriptive group comparisons, mean difference tests, and long-difference panel regressions to study the association between inflation risk and country characteristics such as trade openness, monetary policy frameworks, and exchange rate regimes. As explained in Section 6 for each individual country characteristic, the consistency of results across these distinct methodologies provides an important robustness check. Country characteristics associated with lower inflation risk in the descriptive analysis—such as greater trade and financial openness, higher central bank independence, and fixed exchange rate regimes—also emerge as significant correlates in the regression analysis. Conversely, commodity-exporting countries consistently exhibit higher inflation risk across all empirical approaches.

Taken together, these robustness exercises indicate that the main results of the paper are not sensitive to specific modeling choices, risk definitions, or empirical methodologies. Instead, they reflect stable and economically meaningful patterns in the evolution of inflation risk across countries and over time.

8 Conclusion

Our study expands the literature on inflation tail risk by moving beyond the traditional focus on developed economies such as the United States and the euro area. By employing a methodology that enables the simultaneous characterization of inflation tail risk across nearly 200 countries, we provide a comprehensive analysis of how inflation risk varies according to diverse economic characteristics. We define inflation risk as the probability that consumer inflation will exceed 5 percent in twelve months—a measure of right tail risk.

Our model, which builds on the dynamic factor model (DFM) with endogenous stochastic volatility of Caldara et al. (2024), is adapted to handle cross-country datasets with missing observations and mixed frequencies. This approach allows for rich dynamics in the conditional densities of observable variables and enables country- and region-specific analysis.

Our findings indicate that inflation risk rose sharply during the recent pandemic, with the probability of global consumer inflation exceeding 5 percent surpassing 50 percent from March 2021 and remaining elevated through April 2023. This marked a significant shift in the predictive density, with global inflation rising above 5 percent in October 2021—a level not seen since the global financial crisis and in earlier decades. The increase in inflation risk was observed across most regions of the world. Additionally, our estimates allow for the assessment of stagflation risk, defined as the joint occurrence of high inflation and negative industrial production growth. We find that global stagflation risk briefly exceeded 50 percent in October 2021, a level not seen since the mid-1990s.

Finally, our analysis of country characteristics reveals that greater trade and capital account openness are associated with lower inflation risk, while commodity exporters face higher risk. The adoption of inflation targeting regimes is linked to reduced inflation risk, particularly in advanced economies, and greater central bank independence and transparency are associated with significantly lower inflation risk. Inflation risk was also lower during monetary policy hiking cycles. Countries with fixed exchange rate regimes also systematically experience lower inflation risk. These insights offer valuable opportunities for further country- and region-specific research and policy analysis.

References

Adrian, T., N. Boyarchenko, and D. Giannone (2019): "Vulnerable Growth," *American Economic Review*, 109, 1263–1289.

Andrieu, C., A. Doucet, and R. Holenstein (2010): "Particle Markov chain Monte Carlo methods," *Journal of the Royal Statistical Society Series B*, 72, 269–342.

Ardakani, O. M., N. K. Kishor, and S. Song (2018): "Re-evaluating the effectiveness of inflation targeting," *Journal of Economic Dynamics and Control*, 90, 76–97.

Banerjee, R., J. Contreras, A. Mehrotra, and F. Zampolli (2024): "Inflation at risk in advanced and emerging market economies," *Journal of International Money and Finance*, 142, 103025.

Bowdler, C. and A. Malik (2005): "Openness and inflation volatility: Cross-country evidence," .

Caldara, D., H. Mumtaz, and M. Zhong (2024): "Risk in a Data-Rich Model," Tech. rep., Federal Reserve Board.

Carter, C. K. and R. Kohn (1994): "On Gibbs sampling for state space models," *Biometrika*, 81, 541–53).

Chan, J. C.-C. and I. Jeliazkov (2009): "MCMC Estimation of Restricted Covariance Matrices," *Journal of Computational and Graphical Statistics*, 18, 457–480.

Chinn, M. D. and H. Ito (2006): "What matters for financial development? Capital controls, institutions, and interactions," *Journal of development economics*, 81, 163–192.

Christensen, J., J. Gamble, and S. Zhu (2020): "Coronavirus and the Risk of Deflation," *FRBSF Economic Letter*, 2020, 1–5.

Christensen, J. H., J. A. Lopez, and G. D. Rudebusch (2016): "Pricing deflation risk with US Treasury yields," *Review of Finance*, 20, 1107–1152.

Creal, D. D. and J. C. Wu (2017): "Monetary Policy Uncertainty and Economic Fluctuations," *International Economic Review*, 58, 1317–54.

Diebold, F. X., A. Tay, and K. Wallis (1997): "Evaluating density forecasts of inflation: the survey of professional forecasters," .

Dincer, N. and B. Eichengreen (2010): "Central bank transparency: Causes, consequences and updates," *Theoretical Inquiries in Law*, 11, 75–123.

Dincer, N. N. and B. Eichengreen (2014): "Central bank transparency and independence: Updates and new measures," *34th issue (March 2014) of the International Journal of Central Banking.*

Engle, R. F. (1982): "Autoregressive conditional heteroscedasticity with estimates of the variance of United Kingdom inflation," *Econometrica: Journal of the econometric society*, 987–1007.

Fleckenstein, M., F. A. Longstaff, and H. Lustig (2017): "Deflation risk," *The Review of Financial Studies*, 30, 2719–2760.

Forbes, K., J. Ha, and M. A. Kose (2024): "Rate cycles," Tech. rep., Working Paper.

Furceri, D., D. Giannone, F. Kisat, W. R. Lam, and H. Li (2025): "Debt-at-Risk," *IMF Working Paper.*

Garrón, I., C. V. Rodríguez-Caballero, and E. Ruiz (2024): "International vulnerability of inflation," *arXiv preprint arXiv:2410.20628.*

Ghosh, A. R., A.-M. Gulde, J. D. Ostry, and H. C. Wolf (1997): "Does the nominal exchange rate regime matter?" .

Granato, J., M. Lo, and M. S. Wong (2006): "Testing monetary policy intentions in open economies," *Southern Economic Journal*, 72, 730–746.

Ha, J., A. Ivanova, F. Ohnsorge, and D. F. Unsal (2019): "Inflation: Concepts, evolution, and correlates," *World Bank Policy Research Working Paper.*

Hilscher, J., A. Raviv, and R. Reis (2024): "How likely is an inflation disaster?" *Review of Financial Studies.*

Jacquier, E., N. G. Polson, and P. E. Rossi (2002): "Bayesian Analysis of Stochastic Volatility Models," *Journal of Business & Economic Statistics*, 20, 69–87.

Kiley, M. T. (2022): "Unemployment risk," *Journal of Money, Credit and Banking*, 54, 1407–1424.

Kilian, L. and S. Manganelli (2007): "Quantifying the risk of deflation," *Journal of Money, Credit and Banking*, 39, 561–590.

Kitsul, Y. and J. H. Wright (2013): "The economics of options-implied inflation probability density functions," *Journal of Financial Economics*, 110, 696–711.

Koop, G., M. H. Pesaran, and S. M. Potter (1996): "Impulse response analysis in nonlinear multivariate models," *Journal of Econometrics*, 74, 119–147.

Lanne, M. and H. Nyberg (2016): "Generalized Forecast Error Variance Decomposition for Linear and Nonlinear Multivariate Models†," *Oxford Bulletin of Economics and Statistics*, 78, 595–603.

Lenza, M., I. Moutachaker, and J. Paredes (2025): "Density forecasts of inflation: A quantile regression forest approach," *European Economic Review*, 105079.

Lindsten, F., M. I. Jordan, and T. B. Schön (2014): "Particle Gibbs with Ancestor Sampling," *Journal of Machine Learning Research*, 15, 2145–2184.

López-Salido, D. and F. Loria (2024): "Inflation at risk," *Journal of Monetary Economics*, 145, 103570, inflation: Expectations Dynamics October 14-15, 2022.

Mankiw, N. G., R. Reis, and J. Wolfers (2003): "Disagreement about inflation expectations," *NBER macroeconomics annual*, 18, 209–248.

Marcellino, M., M. Porqueddu, and F. Venditti (2016): "Short-Term GDP Forecasting With a Mixed-Frequency Dynamic Factor Model With Stochastic Volatility," *Journal of Business & Economic Statistics*, 34, 118–127.

Moreno, R. (2001): "Pegging and stabilization policy in developing countries," *Economic Review-Federal Reserve Bank of San Francisco*, 17–30.

Mumtaz, H. (2018): "A Generalised Stochastic Volatility in Mean VAR," *Economics Letters*, 173, 10–14.

Mumtaz, H. and F. Zanetti (2013): "The Impact of the Volatility of Monetary Policy Shocks," Journal of Money Credit and Banking Forthcoming, Bank of England.

Queyranne, M. M., R. Lafarguette, and K. Johnson (2022): *Inflation-at-Risk in in the Middle East, North Africa, and Central Asia*, 2022-2168, International Monetary Fund.

Shambaugh, J. C. (2004): "The effect of fixed exchange rates on monetary policy," *the Quarterly Journal of economics*, 119, 301–352.

Shin, M. and M. Zhong (2020): "A New Approach to Identifying the Real Effects of Uncertainty Shocks," *Journal of Business & Economic Statistics*, 38, 367–79.

Stock, J. H. and M. W. Watson (1999): "Forecasting inflation," *Journal of Monetary Economics*, 44, 293–335.

——— (2002): "Macroeconomic Forecasting Using Diffusion Indexes," *Journal of Business & Economic Statistics*, 20, 147–162.

Stojanovikj, M. and G. Petrevski (2021): "Macroeconomic effects of inflation targeting in emerging market economies," *Empirical Economics*, 61, 2539–2585.

Figure 10: Correlates of inflation risk: Economic structure

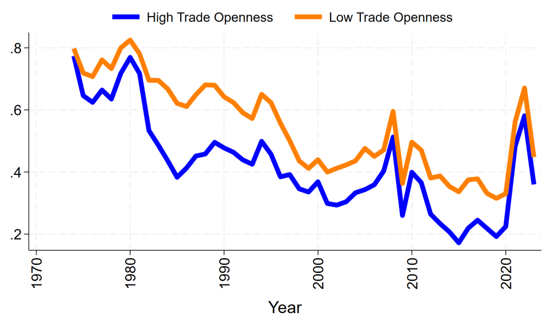

(a) Inflation risk by country groups

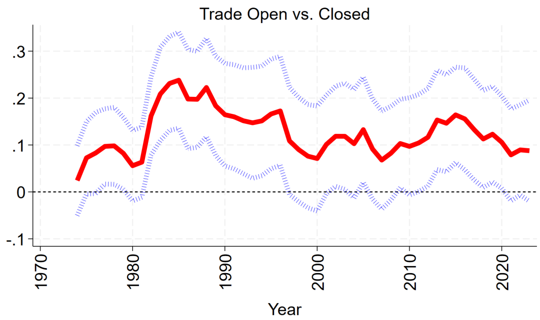

(b) Differences in inflation risk

(A) Trade Openness

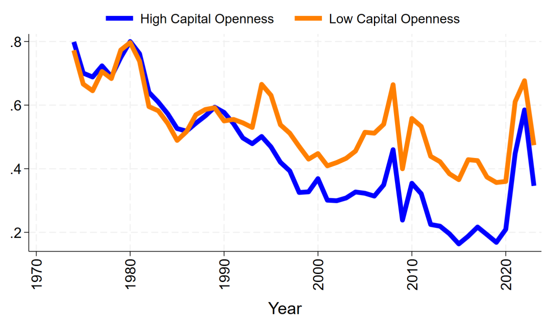

(a) Inflation risk by country groups

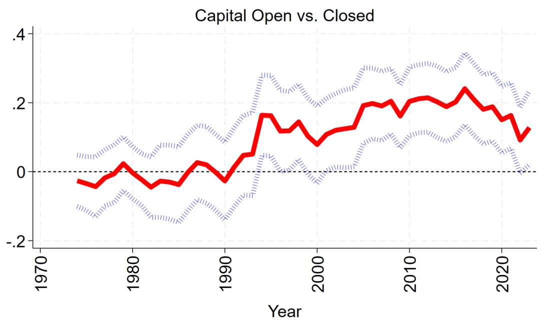

(b) Differences in inflation risk

(B) Capital openness

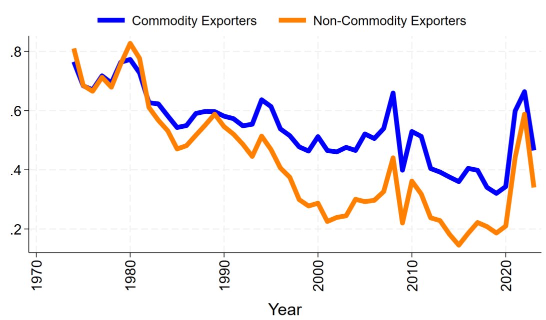

(a) Inflation risk by country groups

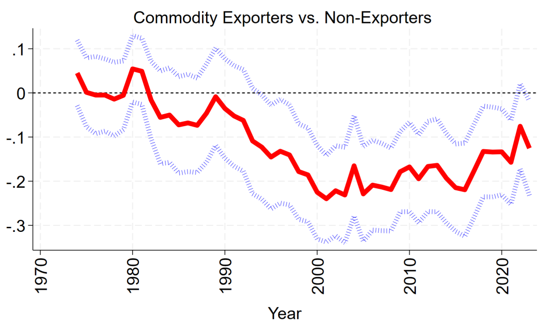

(b) Differences in inflation risk

(C) Commodity Exporters

Note: Computed inflation risk and the differences in inflation risk estimates for various structural economic characteristics, as summarized in Table A.2 The left figures indicate average inflation risk within each group of countries at each period. Red liens in the right figures shows the differences in inflation risks by two country groups, along with 5th-95th confidence intervals (gray lines).

Figure 11: Correlates of inflation risk: Policy framework

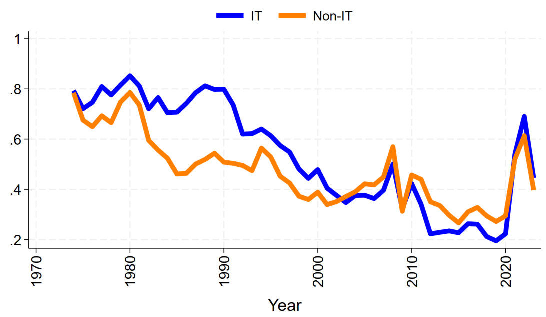

(a) Inflation risk by country groups

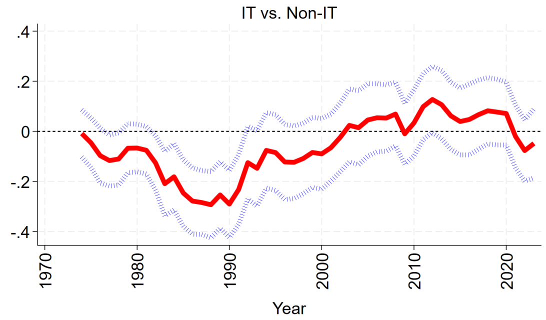

(b) Differences in inflation risk

(A) Inflation Targeting

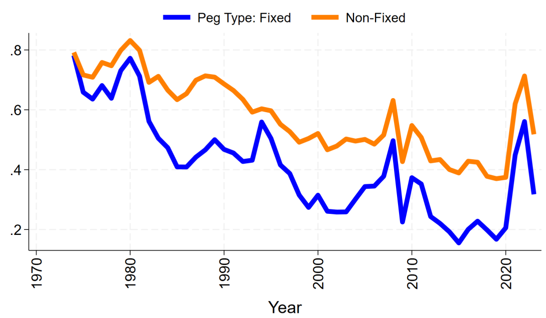

(a) Inflation risk by country groups

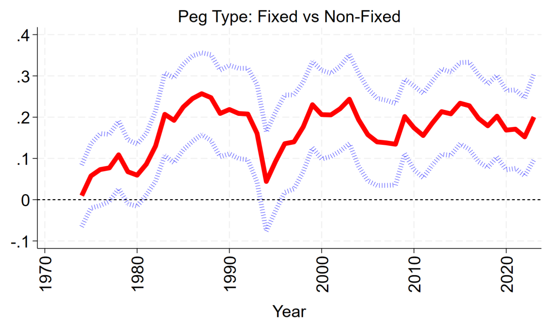

(b) Differences in inflation risk

(B) Pegged Exchange Rate Regime

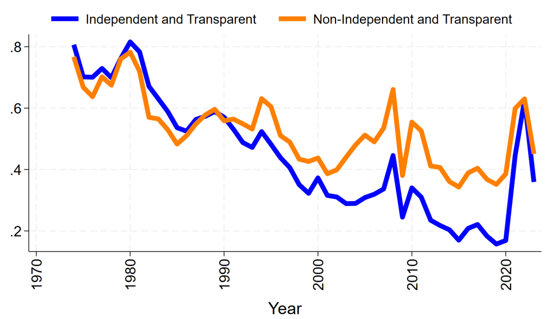

(a) Inflation risk by country groups

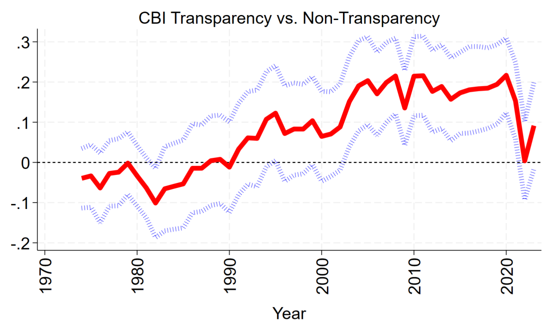

(b) Differences in inflation risk

(C) Central Bank Independence and Transparency

Note: Computed inflation risk and the differences in inflation risk estimates for various structural economic characteristics, as summarized in Table A.2. The left figures indicate average inflation risk within each group of countries at each period. Red liens in the right figures shows the differences in inflation risks by two country groups, along with 5th-95th confidence intervals (gray lines).

A1 Appendix

A1.1 Details of the Gibbs algorithm

The Gibbs sampling algorithm used to estimate the model is identical to that introduced in Caldara et al. (2024) apart from the steps to draw the factors and factor loadings. This is because our data consists of missing values and features mixed-frequencies. We provide details of these steps in this appendix and refer the reader to Caldara et al. (2024) for the remainder.

1. Latent factors , $G(F_t|\Theta)$**.** Conditional on the remaining parameters Θ and the stochastic volatilities $\tilde{h}_t, \tilde{r}_t$, the conditional posterior distribution of F_t is Gaussian. The model can be written as a linear state-space model where the measurement equation changes over time depending on the presence of missing observations. We define the following state vector:

$$Z_t = \begin{pmatrix} \tilde{h}_{t+1} \\ z_t \\ f_t \\ \tilde{h}_t \\ z_{t-1} \\ f_{t-1} \\ \tilde{h}_{t-1} \\ z_{t-2} \\ f_{t-2} \\ v_{j,t} \\ v_{j,t-1} \\ v_{j,t-2} \vdots \end{pmatrix} \tag{10}$$

where v_j denotes the idiosyncratic components for series with missing values. Note that $\tilde{h_{t+1}}, z_t$ are observed states and appear on both sides of the measurement equation (identities). In general, the measurement equation is:

$$\begin{aligned} \tilde{X}_{it} &= \tilde{B} Z_t + V_t, \\ var(V_t) &= R_{F,t} \end{aligned}$$

Note that the top $N + N_z$ rows of $\tilde{X}_{it}$ consist of $\begin{pmatrix} \tilde{h}_{t+1} \\ z_t \end{pmatrix}$ At each point in time, the matrices of the observation equation are built series by series and change depending on the presence of mixed frequencies or missing values. To demonstrate this, we consider an example where $T = 3$ and the panel consists of 3 series: X_1 which has no missing values, X_3 that is quarterly and only observed in period 3 and X_2 that has a missing value in period 1 and available elsewhere. We also assume that the idiosyncratic shocks follow and AR(1) process. First consider the case in period 1 of the sample. Then the measurement equation is:

$$\begin{pmatrix} \tilde{h}_{t+1} \\ z_t \\ X_{1,t} - \rho_i X_{1,t-1} \\ nan \\ nan \end{pmatrix} = \begin{pmatrix} 1 & 0 & 0 & 0 & 0 & 0 & 0 & 0 & 0 & 0 & 0 & 0 & 0 \\ 0 & 1 & 0 & 0 & 0 & 0 & 0 & 0 & 0 & 0 & 0 & 0 & 0 \\ 0 & B_{1,z} & B_{1,f} & 0 & -\rho B_{1,z} & -\rho B_{1,z} & 0 & 0 & 0 & 0 & 0 & 0 & 0 \\ 0 & 0 & 0 & 0 & 0 & 0 & 0 & 0 & 0 & 0 & 0 & 0 & 0 \\ 0 & 0 & 0 & 0 & 0 & 0 & 0 & 0 & 0 & 0 & 0 & 0 & 0 \end{pmatrix} \begin{pmatrix} \tilde{h}_{t+1} \\ z_t \\ f_t \\ \tilde{h}_t \\ z_{t-1} \\ f_{t-1} \\ \tilde{h}_{t-1} \\ z_{t-2} \\ f_{t-2} \\ v_{2,t} \\ v_{3,t} \\ v_{3,t-1} \\ v_{3,t-2} \end{pmatrix}$$

$$+ \begin{pmatrix} 0 \\ 0 \\ u_{1t} \\ u^*_{2,t} \\ u^*_{3,t} \end{pmatrix}$$

where $var(u_{1t}) = r_{1t}$ while $var(u^*_{2,t}1e5) = var(u^*_{2,t}) = 1e5$. In period 2, the observation equation is as follows. Note the change in the equation for $X_{2,t}$

$$
\begin{pmatrix} \tilde{h}_{t+1} \\ z_t \\ X_{1,t} - \rho_i X_{1,t-1} \\ X_{2,t} \\ nan \end{pmatrix} = \begin{pmatrix} 1 & 0 & 0 & 0 & 0 & 0 & 0 & 0 & 0 & 0 & 0 & 0 & 0 \\ 0 & 1 & 0 & 0 & 0 & 0 & 0 & 0 & 0 & 0 & 0 & 0 & 0 \\ 0 & B_{1,z} & B_{1,f} & 0 & -\rho B_{1,z} & -\rho B_{1,z} & 0 & 0 & 0 & 0 & 0 & 0 & 0 \\ 0 & B_{2,z} & B_{2,f} & 0 & 0 & 0 & 0 & 0 & 0 & 1 & 0 & 0 & 0 \\ 0 & 0 & 0 & 0 & 0 & 0 & 0 & 0 & 0 & 0 & 0 & 0 & 0 \end{pmatrix} \begin{pmatrix} \tilde{h}_{t+1} \\ z_t \\ f_t \\ \tilde{h}_t \\ z_{t-1} \\ f_{t-1} \\ \tilde{h}_{t-1} \\ z_{t-2} \\ f_{t-2} \\ v_{2,t} \\ v_{3,t} \\ v_{3,t-1} \\ v_{3,t-2} \end{pmatrix}
$$

$$
+ \begin{pmatrix} 0 \\ 0 \\ u_{1t} \\ 0 \\ u^*_{3,t} \end{pmatrix}
$$

In period 3, the observation equation is as follows. Note the change in the equation for $X_{3,t}$ as data is observed at the end of the quarter.

$$
\begin{pmatrix} \tilde{h}_{t+1} \\ z_t \\ X_{1,t} - \rho_i X_{1,t-1} \\ X_{2,t} \\ X_{3,t} \end{pmatrix} = \begin{pmatrix} 1 & 0 & 0 & 0 & 0 & 0 & 0 & 0 & 0 & 0 & 0 & 0 & 0 \\ 0 & 1 & 0 & 0 & 0 & 0 & 0 & 0 & 0 & 0 & 0 & 0 & 0 \\ 0 & B_{1,z} & B_{1,f} & 0 & -\rho B_{1,z} & -\rho B_{1,z} & 0 & 0 & 0 & 0 & 0 & 0 & 0 \\ 0 & B_{2,z} & B_{2,f} & 0 & 0 & 0 & 0 & 0 & 0 & 1 & 0 & 0 & 0 \\ 0 & \frac{B_{3,z}}{3} & \frac{B_{3,f}}{3} & 0 & \frac{B_{3,z}}{3} & \frac{B_{3,f}}{3} & 0 & \frac{B_{3,z}}{3} & \frac{B_{3,f}}{3} & 0 & 1 & 1 & 1 \end{pmatrix} \begin{pmatrix} \tilde{h}_{t+1} \\ z_t \\ f_t \\ \tilde{h}_t \\ z_{t-1} \\ f_{t-1} \\ \tilde{h}_{t-1} \\ z_{t-2} \\ f_{t-2} \\ v_{2,t} \\ v_{3,t} \\ v_{3,t-1} \\ v_{3,t-2} \end{pmatrix}
$$

$$+\begin{pmatrix} 0 \\ 0 \\ u_{1t} \\ 0 \\ 0 \end{pmatrix}$$

The transition equation for the model in this example is:

$$\begin{pmatrix} \tilde{h}_{t+1} \\ z_t \\ f_t \\ \tilde{h}_t \\ z_{t-1} \\ f_{t-1} \\ \tilde{h}_{t-1} \\ z_{t-2} \\ f_{t-2} \\ v_{2,t} \\ v_{3,t} \\ v_{3,t-1} \\ v_{3,t-2} \end{pmatrix} = \begin{pmatrix} \alpha \\ c_z \\ c_f \\ 0 \\ 0 \\ 0 \\ 0 \\ 0 \\ 0 \\ 0 \\ 0 \\ 0 \\ 0 \end{pmatrix} + \begin{pmatrix} \theta & d_{z,1} & d_{f,1} & 0 & 0 & 0 & 0 & 0 & 0 & 0 & 0 & 0 & 0 \\ 0 & \beta_{z,1,1} & \beta_{f,1,1} & b_{1,1} & 0 & 0 & 0 & 0 & 0 & 0 & 0 & 0 & 0 \\ 0 & \beta_{z,2,1} & \beta_{f,2,1} & b_{2,1} & 0 & 0 & 0 & 0 & 0 & 0 & 0 & 0 & 0 \\ 1 & 0 & 0 & 0 & 0 & 0 & 0 & 0 & 0 & 0 & 0 & 0 & 0 \\ 0 & 1 & 0 & 0 & 0 & 0 & 0 & 0 & 0 & 0 & 0 & 0 & 0 \\ 0 & 0 & 1 & 0 & 0 & 0 & 0 & 0 & 0 & 0 & 0 & 0 & 0 \\ 0 & 0 & 0 & 1 & 0 & 0 & 0 & 0 & 0 & 0 & 0 & 0 & 0 \\ 0 & 0 & 0 & 0 & 1 & 0 & 0 & 0 & 0 & 0 & 0 & 0 & 0 \\ 0 & 0 & 0 & 0 & 0 & 1 & 0 & 0 & 0 & 0 & 0 & 0 & 0 \\ 0 & 0 & 0 & 0 & 0 & 0 & 0 & 0 & 0 & \rho_2 & 0 & 0 & 0 \\ 0 & 0 & 0 & 0 & 0 & 0 & 0 & 0 & 0 & 0 & \rho_3 & 0 & 0 \\ 0 & 0 & 0 & 0 & 0 & 0 & 0 & 0 & 0 & 0 & 1 & 0 & 0 \\ 0 & 0 & 0 & 0 & 0 & 0 & 0 & 0 & 0 & 0 & 0 & 1 & 0 \end{pmatrix} \begin{pmatrix} \tilde{h}_t \\ z_{t-1} \\ f_{t-1} \\ \tilde{h}_{t-1} \\ z_{t-2} \\ f_{t-2} \\ \tilde{h}_{t-2} \\ z_{t-3} \\ f_{t-3} \\ v_{2,t-1} \\ v_{3,t-1} \\ v_{3,t-2} \\ v_{3,t-3} \end{pmatrix} + \begin{pmatrix} \tilde{\eta}_t \\ e_{zt} \\ e_{ft} \\ 0 \\ 0 \\ 0 \\ 0 \\ 0 \\ 0 \\ u_{2t} \\ u_{3t} \\ 0 \\ 0 \end{pmatrix}$$

where:

$$var\begin{pmatrix} \tilde{\eta}_t \\ e_t \end{pmatrix} = \Omega_t = \begin{pmatrix} S^{1/2} & 0 \\ 0 & H_t^{1/2} \end{pmatrix} \begin{pmatrix} \Sigma_\eta & \Sigma'_{\eta_t e_t} \\ \Sigma_{\eta_t e_t} & \Sigma_{e_t} \end{pmatrix} \begin{pmatrix} S^{1/2} & 0 \\ 0 & H_t^{1/2} \end{pmatrix}'$$

with $e_t = \begin{pmatrix} e_{zt} \\ e_{ft} \end{pmatrix}$ and $var(u_{2t}) = r_{2t}$ and $var(u_{3t}) = r_{3t}$. The model in state-space form is linear and conditionally Gaussian. We draw from the conditional posterior distribution of the factors using the Carter and Kohn (1994) algorithm.

2. Factor loadings, $G(B|\Theta)$**.** For series in X_t with no missing values, the factor loadings are coefficients in linear regressions with serial correlation and heteroscedasticity and their conditional posterior is standard after a GLS transformation (see Caldara et al. (2024)). When the ith series X_{it} has data missing at random or is observed at a lower frequency, we draw the factor loadings using a random walk Metropolis Hastings step.

Note that, conditional on F_t, the model is given by:

$$X_{it}^{Q} = \frac{B_f}{3}\sum_{j=0}^{2} f_{t-j} + \frac{B_z}{3}\sum_{j=0}^{2} z_{t-j} + \sum_{j=0}^{2} v_{it-j} \text{ quarterly data} \tag{11}$$

$$X_{it}^{-Y} = u_{it} \text{ missing data} \tag{12}$$

$$X_{it} = B_f f_t + B_z z_t + v_{it} \text{ monthly data} \tag{13}$$

Our proposal distribution is the mixture density $q(B_i) \sim N\left(B_i^{old}, \varpi\right)$ where B_i^{old} denotes the previous draw and the variance ϖ is set to achieve a reasonable acceptance rate. The candidate draw B_i^{new} is accepted with probability:

$$\alpha = \min\left(\frac{f\left(X_{it}|B_i^{new}\right)p\left(B_i^{new}\right)}{f\left(X_{it}|B_i^{old}\right)p\left(B_i^{old}\right)}, 1\right)$$

where $f(X_{it}|B_i)$ denotes the likelihood and $p(B_i)$ is the prior. To calculate the likelihood, we use the Kalman filter to accommodate the moving average error term in 11. The observation equation of the system is given by equations 11 to 13 where the terms $\frac{B_f}{3}\sum_{j=0}^{2} f_{t-j} + \frac{B_z}{3}\sum_{j=0}^{2} z_{t-j}$ and $B_f f_t + B_z z_t$ are treated as known and $var(u_{it}) = 1e10$. The transition equation of the system is:

$$\begin{pmatrix} v_{1t} \\ v_{1t-1} \\ v_{1t-2} \end{pmatrix} = \begin{pmatrix} \rho & 0 & 0 \\ 1 & 0 & 0 \\ 0 & 1 & 0 \end{pmatrix} \begin{pmatrix} v_{1t-1} \\ v_{1t-2} \\ v_{1t-3} \end{pmatrix} + \begin{pmatrix} r_{it}^{1/2}\varepsilon_{it} \\ 0 \\ 0 \end{pmatrix}$$

A1.2 Model with more factors

To check the robustness of the benchmark results we re-estimate the model increasing setting $N_f = 4$ and $N_z = 6$. Figures A.1 and A.2 compare the estimated global and regional risk measures to those obtained from the benchmark model (black line). Adding extra factors does not alter the main conclusions substantially.

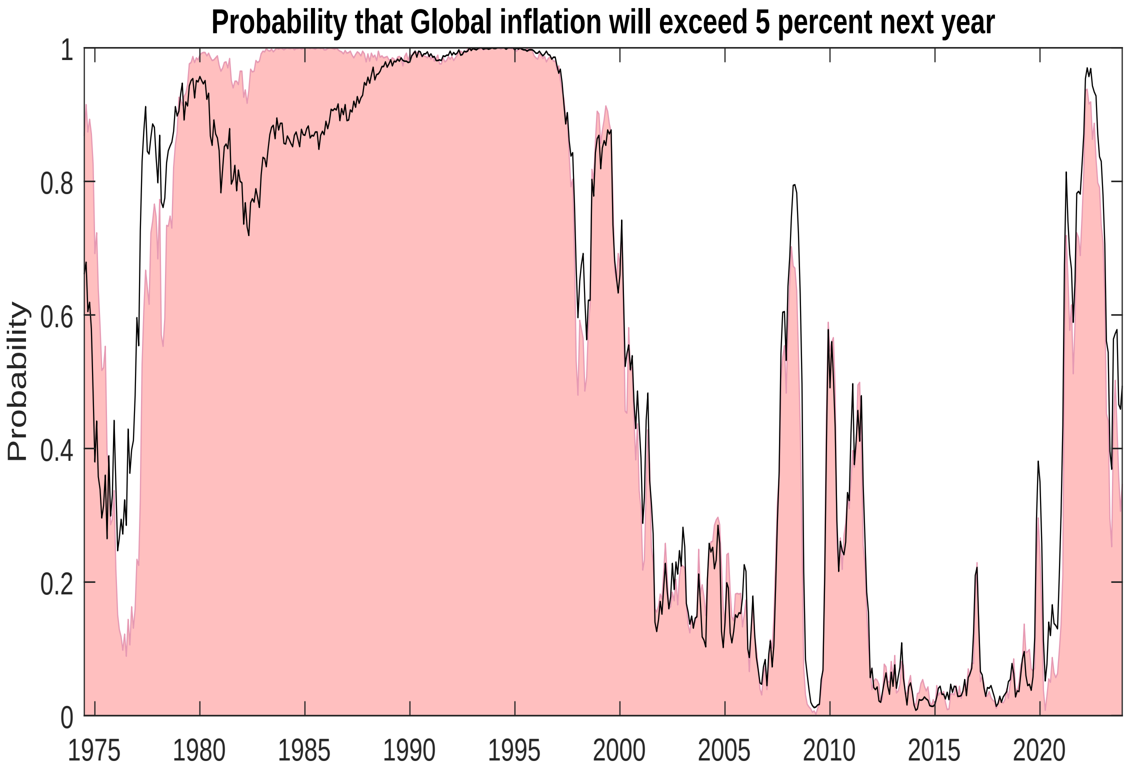

Figure A.1: The probability that Global inflation will exceed 5% one year ahead. The black line is the estimate from the benchmark model.

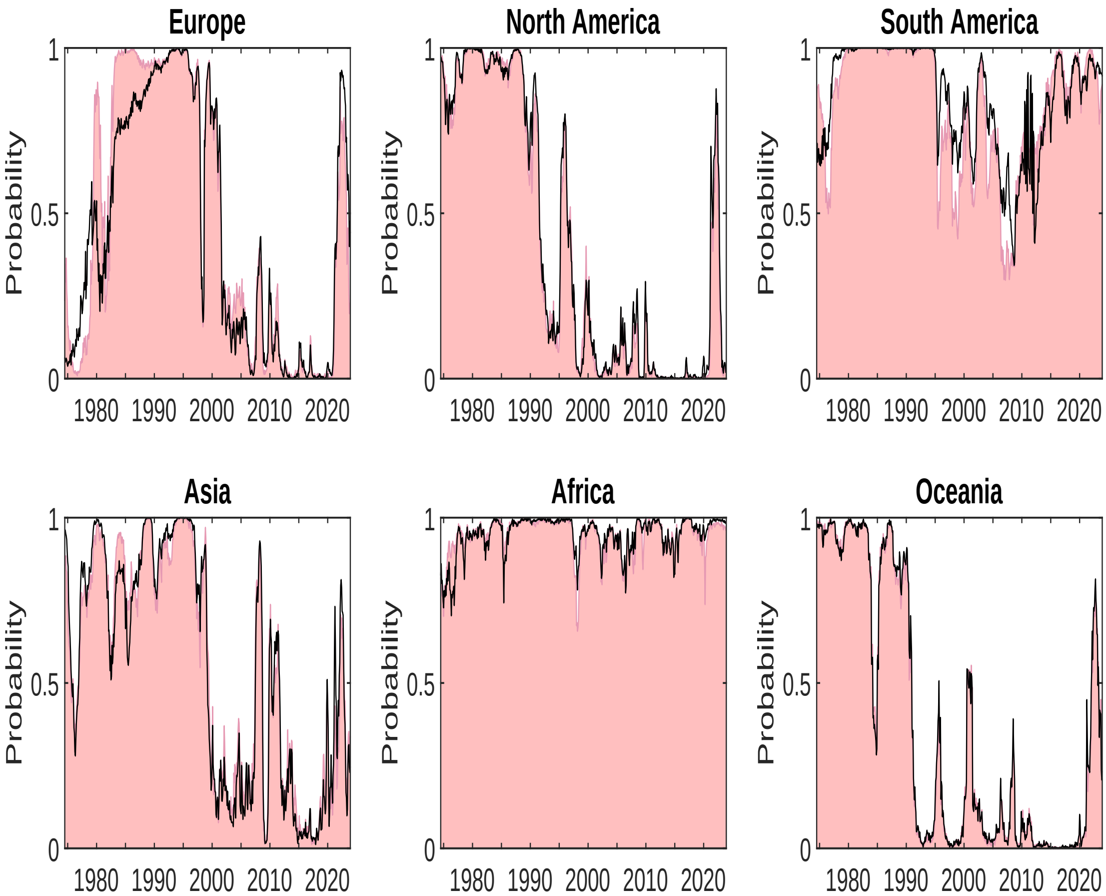

Figure A.2: The probability that Regional inflation will exceed 5% one year ahead. The black line is the estimate from the benchmark model.

A1.3 Impulse responses of IP and inflation measures

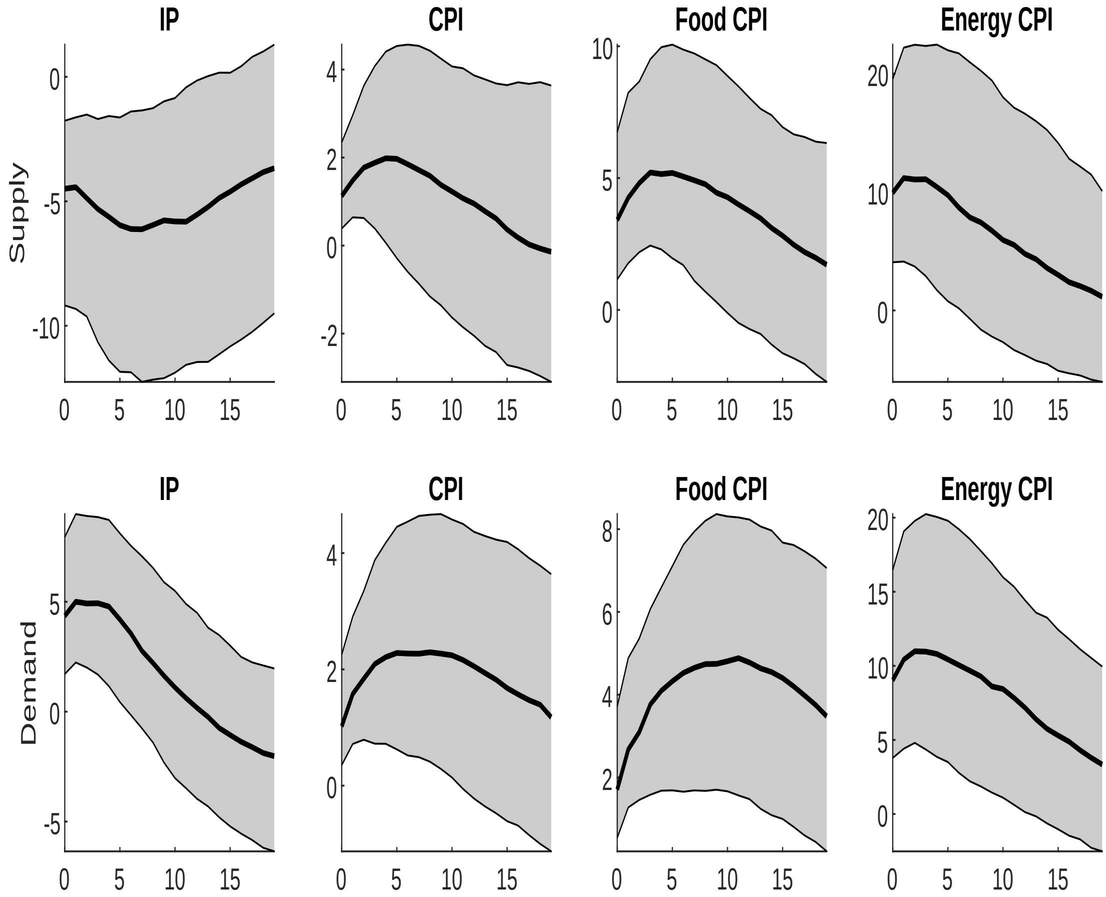

Figure A.3: Impulse response of global aggregates to supply and demand shocks. Aggregates are weighted averages computed using PPP weights

A1.4 Data

Available sample for variables in X_t. Start date and end date shown. M (Q) denotes monthly (quarterly) data.

	CPI	IP		CPI	IP
ABW	01/87-02/20-M	nan	AFG	03/05-03/20-M	nan
AGO	01/92-12/23-M	nan	AIA	12/91-09/23-Q	nan
ALB	01/92-08/23-M	nan	ANT	03/71-12/15-Q	nan
ARE	01/08-12/22-M	nan	ARG	01/71-03/23-M	01/17-08/23-M
ARM	12/93-12/23-M	nan	ATG	11/93-02/23-M	nan
AUS	03/71-12/23-Q	nan	AUT	01/71-12/23-M	01/06-08/23-M
AZE	01/93-12/23-M	nan	BDI	01/75-12/23-M	nan
BEL	01/71-12/23-M	01/01-07/23-M	BEN	12/92-06/23-M	nan
BFA	01/71-12/23-M	nan	BGD	07/94-10/23-M	nan
BGR	01/92-12/23-M	01/01-08/23-M	BHR	07/76-11/23-M	nan
BHS	07/73-11/23-M	nan	BIH	01/06-02/23-M	04/13-08/23-M
BLR	01/92-12/23-M	01/09-08/23-M	BLZ	02/91-02/23-M	nan
BOL	01/71-12/23-M	nan	BRA	12/80-12/23-M	01/03-08/23-M
BRB	01/71-10/23-M	nan	BRN	01/85-12/23-M	nan
BTN	12/80-09/23-Q	nan	BWA	06/76-12/23-M	nan
CAF	01/82-03/23-M	nan	CAN	01/71-12/23-M	01/82-07/23-M
CHE	01/71-12/23-M	nan	CHL	01/71-12/23-M	01/10-08/23-M
CHN	01/87-12/23-M	01/98-08/23-M	CIV	01/71-12/23-M	nan
CMR	01/71-12/23-M	nan	COD	01/71-02/17-M	nan
COG	01/91-12/23-M	nan	COL	01/71-12/23-M	nan
COM	12/00-10/14-M	nan	CPV	01/93-11/23-M	nan
CRI	01/71-12/23-M	nan	CUW	01/01-02/20-M	nan
CYM	06/09-12/16-Q	nan	CYP	01/71-12/23-M	01/01-07/23-M
CZE	01/92-12/23-M	01/01-08/23-M	DEU	01/71-12/23-M	01/71-08/23-M
DJI	01/82-01/23-M	nan	DMA	01/71-09/23-M	nan
DNK	01/71-12/23-M	01/01-08/23-M	DOM	01/71-12/23-M	nan
DZA	01/75-12/23-M	nan	ECU	01/71-12/23-M	nan
EGY	01/71-12/23-M	07/07-07/23-M	ESP	01/71-12/23-M	01/93-08/23-M
EST	01/99-12/23-M	01/01-08/23-M	ETH	01/71-06/23-M	nan
FIN	01/71-12/23-M	01/96-08/23-M	FJI	01/71-09/23-M	nan
FRA	01/71-12/23-M	01/71-08/23-M	FRO	03/02-12/23-Q	nan
FSM	12/99-12/22-Q	nan	GAB	01/71-12/23-M	nan
GBR	01/71-12/23-M	01/71-07/23-M	GEO	01/95-12/23-M	nan
GHA	01/71-12/23-M	nan	GIN	01/05-12/23-M	nan
GLP	03/11-12/16-Q	nan	GMB	01/71-12/23-M	nan

Continued on next page

Table A.1 – Continued from previous page

	CPI	IP		CPI	IP
GNB	02/87-04/23-M	nan	GNQ	01/86-05/23-M	nan
GRC	01/71-12/23-M	01/96-08/23-M	GRD	01/77-12/21-M	nan
GTM	01/71-03/23-M	nan	GUY	01/95-12/23-M	nan
HKG	10/81-03/23-M	nan	HND	01/71-12/23-M	nan
HRV	01/87-12/23-M	01/99-08/23-M	HTI	01/71-10/23-M	nan
HUN	01/81-12/23-M	01/94-08/23-M	IDN	01/71-12/23-M	nan
IND	01/71-12/23-M	nan	IOT	nan	01/72-07/23-M
IRL	01/71-12/23-M	01/81-08/23-M	IRN	01/71-05/22-M	nan
IRQ	01/08-11/23-M	nan	ISL	01/71-12/23-M	nan
ISR	01/71-12/23-M	nan	ITA	01/71-12/23-M	01/81-08/23-M
JAM	01/71-11/23-M	nan	JEY	03/90-12/23-Q	nan
JOR	01/77-12/23-M	01/03-07/23-M	JPN	01/71-12/23-M	01/09-08/23-M
KAZ	12/93-03/23-M	12/99-08/23-M	KEN	01/71-02/23-M	nan
KGZ	01/96-12/23-M	nan	KHM	10/95-12/23-M	nan
KIR	01/07-03/20-M	nan	KNA	01/79-09/23-M	nan
KOR	01/71-12/23-M	01/81-08/23-M	KWT	01/74-12/23-M	nan
LAO	12/88-12/23-M	nan	LBN	12/08-12/23-M	nan
LBR	01/02-02/19-M	nan	LBY	01/71-05/14-M	nan
LCA	01/71-12/22-M	nan	LIE	01/12-12/21-M	nan
LKA	01/71-12/23-M	01/11-07/23-M	LSO	01/03-12/23-M	nan
LTU	12/91-12/23-M	01/99-08/23-M	LUX	01/71-12/23-M	01/71-07/23-M
LVA	01/92-12/23-M	01/01-08/23-M	MAC	01/89-01/23-M	nan
MAR	01/71-12/23-M	nan	MDA	01/92-10/23-M	nan
MDG	01/71-01/23-M	nan	MDV	01/86-11/23-M	nan
MEX	01/71-12/23-M	nan	MKD	01/94-12/23-M	nan
MLI	07/88-12/23-M	nan	MLT	01/71-12/23-M	01/01-08/23-M
MMR	01/71-11/20-M	nan	MNE	01/06-12/23-M	nan
MNG	01/92-12/23-M	12/20-08/23-M	MOZ	01/05-12/23-M	nan
MRT	07/86-12/22-M	nan	MSR	07/05-03/19-M	nan
MTQ	03/01-06/18-Q	nan	MUS	01/71-12/23-M	nan
MWI	01/81-12/23-M	nan	MYS	01/71-10/23-M	01/16-07/23-M
NAM	01/03-12/23-M	nan	NCL	01/94-11/22-M	nan
NER	01/71-12/23-M	nan	NGA	01/71-09/23-M	nan
NIC	01/00-11/23-M	nan	NIU	03/12-12/23-Q	nan
NLD	01/71-12/23-M	01/01-08/23-M	NOR	01/71-12/23-M	01/71-08/23-M
NPL	01/71-12/23-M	nan	NZL	03/71-12/23-Q	nan
OMN	01/02-03/23-M	nan	PAK	01/71-12/23-M	nan
PAN	07/75-12/23-M	nan	PER	01/71-12/23-M	nan
PHL	01/71-12/23-M	nan	PLW	06/01-12/23-Q	nan

Continued on next page

Table A.1 – Continued from previous page

	CPI	**IP**		**CPI**	**IP**
PNG	03/72-06/23-Q	nan	POL	01/90-12/23-M	02/00-08/23-M
PRI	01/85-06/22-M	nan	PRT	01/71-12/23-M	01/06-08/23-M
PRY	01/71-12/23-M	nan	PSE	01/97-12/23-M	nan
QAT	12/03-12/23-M	nan	ROU	10/91-12/23-M	01/01-07/23-M
RUS	01/93-03/22-M	12/06-08/23-M	RWA	01/71-12/23-M	nan
SAU	02/81-12/23-M	nan	SDN	01/71-02/23-M	nan
SEN	01/71-10/23-M	nan	SGP	01/71-12/23-M	nan
SHN	12/95-12/23-Q	nan	SLB	01/79-01/23-M	nan
SLE	01/07-12/23-M	nan	SLV	01/71-12/23-M	01/06-07/23-M
SMR	03/04-09/18-Q	nan	SRB	02/95-12/23-M	01/95-08/23-M
SSD	04/08-12/23-M	nan	STP	12/97-03/23-M	nan
SUR	01/71-11/23-M	nan	SVK	01/92-12/23-M	01/99-08/23-M
SVN	01/81-12/23-M	01/99-08/23-M	SWE	01/71-12/23-M	01/01-08/23-M
SWZ	01/71-09/20-M	nan	SXM	03/06-12/17-Q	nan
SYC	01/71-10/21-M	nan	SYR	01/71-10/13-M	nan
TCD	02/84-06/23-M	nan	TGO	01/71-01/23-M	nan
THA	01/71-03/23-M	nan	TJK	01/01-12/22-M	nan
TKL	03/13-06/22-Q	nan	TLS	12/02-05/20-M	nan
TON	01/91-09/23-M	nan	TTO	01/71-09/23-M	nan
TUN	07/88-09/23-M	nan	TUR	01/71-12/23-M	01/87-08/23-M
TWN	01/71-03/23-M	nan	TZA	03/79-10/23-M	nan
UGA	03/93-12/23-M	nan	UKR	01/93-12/23-M	01/07-03/23-M
URY	01/71-12/23-M	nan	USA	01/71-12/23-M	01/71-08/23-M
UZB	01/11-05/23-M	nan	VCT	01/76-12/22-M	nan
VEN	12/08-12/16-M	nan	VGB	01/17-08/21-M	nan
VNM	01/96-12/23-M	nan	VUT	03/77-06/23-Q	nan
WSM	01/71-12/23-M	nan	XKX	05/03-12/23-M	nan
YEM	07/98-12/15-M	nan	ZAF	01/71-12/23-M	nan
ZMB	01/86-12/22-M	nan	ZWE	01/10-08/23-M	nan

Table A.2: Dataset for Country Characteristics

Characteristics	Measures	Description
Trade Openness	Trade to GDP	Sum of exports and imports of goods and services as percent of GDP
Financial Openness	Chinn-Ito Index	De jure financial openness as in Chinn and Ito (2006)
Commodity Exporter	Commodity importer and exporter status	An economy is defined as commodity exporter when, either (i) total commodities exports accounted for 30% or more of total goods exports or (ii) exports of any single commodity accounted for 20% or more of total goods exports. All other countries are considered commodity importers.
	Net energy importer	Net fuel imports, defined as fuel imports minus fuel exports as percent of GDP
CBI and Transparency	Central Bank Independence and Transparency	Index as in Dincer and Eichengreen (2010)
Exchange Rate Flexibility	De facto exchange rate regime	Dummy variable; 1 = fixed; 0 = not fixed (From Shambaugh (2004))
Inflation Target	Inflation targeting status	Dummy variable; 1 = inflation targeting; 0 = not inflation targeting
Global Value Chain	Trade integration status	Dummy variable; 1=highly integrated ; 0=not highly integrated

Note: All the data is obtained from the World Bank inflation database compiled by Ha et al. (2019).

A1.5 Results on cross-country heterogeneity in inflation risk

Table A.3: Correlates of changes in Inflation Risk

	(1)	(2)	(3)	(4)	(5)	(6)
Panel A: All Countries						
IT	−0.064					
	(0.078)					
Pegged ER		−0.157***				
		(0.052)				
Commodity Exporter			0.175***			
			(0.052)			
CBI and Transparency				−0.156***		
				(0.053)		
Δ Trade Openness (percent of GDP)					−0.0006**	
					(0.0003)	
Δ Capital Openness Index (point increase)						−0.282***
						(0.094)
Constant	−0.338***	−0.275***	−0.439***	−0.277***	−0.384***	−0.374***
	(0.028)	(0.038)	(0.035)	(0.036)	(0.032)	(0.35)
Observations	192	192	192	192	146	122
R-squared	0.004	0.043	0.054	0.043	0.014	0.095
Panel B: EMDEs						
IT	0.068					
	(0.085)					
Pegged ER		−0.190***				
		(0.057)				
Commodity Exporter			0.113**			
			(0.059)			
CBI and Transparency				−0.015		
				(0.059)		
Δ Trade Openness (percent of GDP)					−0.0007***	
					(0.0003)	
Δ Capital Openness Index (point increase)						−0.077
						(0.111)
Constant	−0.287***	−0.346***	−0.270***	−0.270***	−0.259***	−0.267***
	(0.031)	(0.041)	(0.030)	(0.039)	(0.024)	(0.028)
Observations	147	147	147	147	118	96
R-squared	0.005	0.070	0.023	0.023	0.021	0.013

Table A.3: Correlates of changes in Inflation Risk (continued)

	(1)	(2)	(3)	(4)	(5)	(6)
Panel C: AEs						
IT	−0.281***					
	(0.074)					
Pegged ER		−0.035				
		(0.715)				
Commodity Exporter			−0.159			
			(0.116)			
CBI and Transparency				−0.361***		
				(0.086)		
Δ Trade Openness					0.002***	
(percent of GDP)					(0.000)	
Δ Capital Openness						−0.270**
Index (point increase)						(0.143)
Constant	−0.524***	−0.575***	−0.572***	−0.626***	−0.817***	−0.653***
	(0.057)	(0.066)	(0.052)	(0.070)	(0.043)	(0.086)
Observations	45	45	45	45	28	26
R-squared	0.000	0.003	0.028	0.025	0.186	0.177

Note: In the regression analysis, inflation risk is modeled as $\Delta\pi_{it} = \alpha + \beta X_{it}$, with robust standard errors. Here, $\Delta\pi_{it}$ represents the country-specific change in inflation risk over time t, and X_{it} denotes the relevant country characteristics, as summarized in Table A.2. Changes in inflation rates are calculated as differences in averages between 1974–79 and 2010–19.

School of Economics and Finance

Queen Mary
University of London

This working paper has been produced by
the School of Economics and Finance at
Queen Mary University of London

School of Economics and Finance
Queen Mary University of London
Mile End Road
London E1 4NS
Tel: +44 (0)20 7882 7356
Fax: +44 (0)20 8983 3580
Web: www.econ.qmul.ac.uk/research/workingpapers/